



The  
University  
Of  
Sheffield.

Automatic Control  
& Systems  
Engineering.

## **MR Fluid Based Haptic Feedback System**

**Samanta Suprio Sujoy**

**Registration Number: - 220181471**

**September, 2023**

**Supervisor: Professor Sanja Dogramadzi**

**A dissertation submitted in partial fulfilment of the requirements for  
the degree of MSc in Robotics.**

## ABSTRACT

Haptic feedback is essential for immersive VR experiences and effective teleoperation. Typically, haptic devices fall into Kinesthetic or cutaneous categories. Kinesthetic devices target large muscle groups, while cutaneous devices manipulate mechanoreceptors under the skin, using pressure and lateral forces. Generating both pressure and lateral forces is a complex task, often requiring intricate mechanisms or vibration-based actuators.

This project aims to create an MR Fluid-based haptic feedback device capable of producing normal and lateral forces on the fingers. MR Fluids, known for their non-Newtonian behaviour and viscosity changes in response to a magnetic field (MR Effect), serve as the core technology. A silicone rubber-based wearable haptic device for the index finger was designed and fabricated. Using a peristaltic pump and an electromagnet, precise lateral and normal forces were generated. The force and torque values were evaluated using a load cell sensor. A feedback system linked to a gripping task performed by a Franka gripper was developed and evaluated. This project advances the field of haptic feedback, offering potential applications in VR, teleoperation, and beyond.

## **ACKNOWLEDGEMENTS**

I want to extend my sincere gratitude to my supervisor Professor Sanja Dogramadzi, for providing me the opportunity to work on this project and for providing continuous guidance throughout the span of the project.

Furthermore, I would like to express my gratitude towards the ACSE tech group for providing 3D prints and technical support.

Finally, I would also like to thank Baslin.A.James and Jiayang Du for providing assistance with the various aspect of the project.

## Contents

Introduction.....	5
Aims and Objectives .....	6
Project management .....	6
Related Work .....	9
Methodology.....	11
Magnetorheological Fluid .....	11
Characteristics of MR Fluids.....	13
Pre Yielding behaviour of MR Fluids .....	13
Post Yielding behaviour of MR Fluids.....	16
Design of the wearable haptic device.....	18
System Overview and circuit diagram .....	23
Implementation.....	24
Experiments and Results.....	26
Evaluation of Normal forces .....	26
Results .....	27
Evaluation of Lateral forces .....	29
Results .....	30
Developing a feedback system for a Franka Gripper.....	34
Results .....	37
Conclusion and Future Work.....	39
References.....	41
Appendix-A.....	45
Self-Review.....	47

## Introduction

Tactile feedback systems are currently under intensive investigation for their application in virtual reality (VR) and teleoperation settings, aiming to deliver immersive and engaging experiences. Sole reliance on visual feedback can be misleading and potentially result in errors and accidents. By incorporating tactile sensations, users can confidently navigate VR and teleoperation environments, exhibiting reduced error rates and a lower likelihood of accidents.

Human body contains numerous sensors to perceive various sensory information such as touch, smell, colour, temperature, and vibration. The sensation of touch, pressure, temperature, and texture are perceived by the tactile receptors present in the various parts of our body. The tactile receptors contain jelly like materials which produce an electrical signal on the nerves when subjected to force or pressure [1]. These signals are interpreted by brain which creates an overall touch picture [1]. According to Dargahi et.al [1], the face, back of the neck, the chest, the upper arm, and the fingers have the most sensitive touch receptors. Sensation from the eyes, nose, mouth, and ear are localized, whereas, the touch sensation contains numerous nerves types and sensing elements creating a whole-body experience [1]. Hence, these characteristics allow humans to determine the bulk properties, mass distribution, texture, shape, and temperature through touch. The touch sensation can also provide complex gravitation and inertial force information and estimate incipient slip [1].

The Somatosensory system deals with cutaneous perception by humans. The mechanoreceptors, which senses pressure and vibration, the thermoreceptors, for sensing temperature, and nociceptors for dealing with pain and damage are part of the Somatosensory system [1]. The glabrous skin, which is the hairless part of the skin, contains lots of nerve

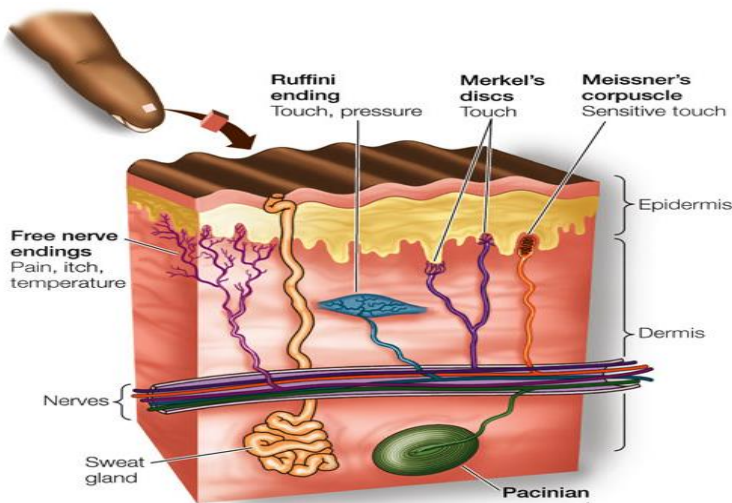


Figure 1: Tactile Receptors on the Human Fingers

endings which makes the area quite sensitive for tactile feedback [1]. The image in Fig 1[2] show the various receptors and their functionality on the glabrous skin.

Tactile feedback can be broadly divided into two types [3]:

1. Kinesthetic Feedback Systems
2. Cutaneous Feedback Systems

As defined by Hong Z. Tan et.al [4], Cutaneous senses are stimulation of the mechanoreceptors, present on the outer surface of the human Body. Whereas, Kinesthetic feedback or Proprioception [4], is manipulation of joint angle position and generation of tension on muscles [4], sensed by the sensory receptors present in the joints and muscles [4].

## Aims and Objectives

The aim of this project is to design, manufacture, and assess a tactile feedback system that utilizes magnetorheological fluid to generate cutaneous feedback.

The various Objectives for completing the aim are explained below:

- To engineer a wearable haptic device with intricate internal veins and strategically placed input/output ports to enable precise fluid flow control for a single finger.
- To develop a system to control and drive the MR fluid using electromagnets, a peristaltic pump, and an Arduino microcontroller board.
- To calculate the viscosity of the MR fluid using the Hagen-Poiseuille equation and compare them against measured values.
- To translate the forces detected by the 6-axis load cell sensor, mounted on a Franka gripper into an effect on the viscosity of the MR Fluid.

## Project management

For successful completion of this project, the objectives were divided into 6 main parts. The first step was conducting a thorough literature review for understanding MR Fluids, Tactile feedback systems and study available technology. Based on the study conducted, the problem statement is formulated. The chart in Fig 2, shows the various parts of the project and the allocated time for each task.

## MAGNETOREHOLOGICAL FLUID BASED TACTILE FEEDBACK SYSTEM

The University of Sheffield  
Samanta Suprio Sujoy

Project Start:

Thu, 2-16-2023

01-01-1900 00:00

Feb 13, 2023

Feb 20, 2023

Feb 27, 2023

Mar 6, 2023

Mar 13, 2023

Mar 20, 2023

Mar 27, 2023

Apr 3, 2023

Apr 10, 2023

Apr 17, 2023

Apr 24, 2023

May 1, 2023

May 8, 2023

May 15, 2023

May 22, 2023

May 29, 2023

Jun 5, 2023

Jun 12, 2023

Jun 19, 2023

Jun 26, 2023

Jul 3, 2023

Jul 10, 2023

Jul 17, 2023

Jul 24, 2023

Jul 31, 2023

Aug 7, 2023

Aug 14, 2023

Aug 21, 2023

Aug 28, 2023

Sep 4, 2023

Sep 11, 2023

Sep 18, 2023



Figure 2: Proposed Gantt Chart

Literature Review was allotted approximately 3 months in total. This period was aimed to understand the functioning of the MR fluids, study haptic feedback systems and understand systems which uses MR Fluids with haptic feedback system. The first step towards fabrication was designing various parts of the wearable haptic device. A total of 50 days were allocated for this task. After designing a prototype, the fabrication and assembly of various electronics components was aimed to be completed in 16 days. The mapping of the haptic system with the Franka Gripper was allotted 21 days. The evaluation of the system was planned to be completed in 40 days. Tracking the progress and logging important findings to generate a technical report was planned to be done along with the assembly, mapping, and system evaluation tasks.

## MAGNETOREHOLOGICAL FLUID BASED TACTILE FEEDBACK SYSTEM

The University of Sheffield

Samanta Suprio Sujoy

Project Start:

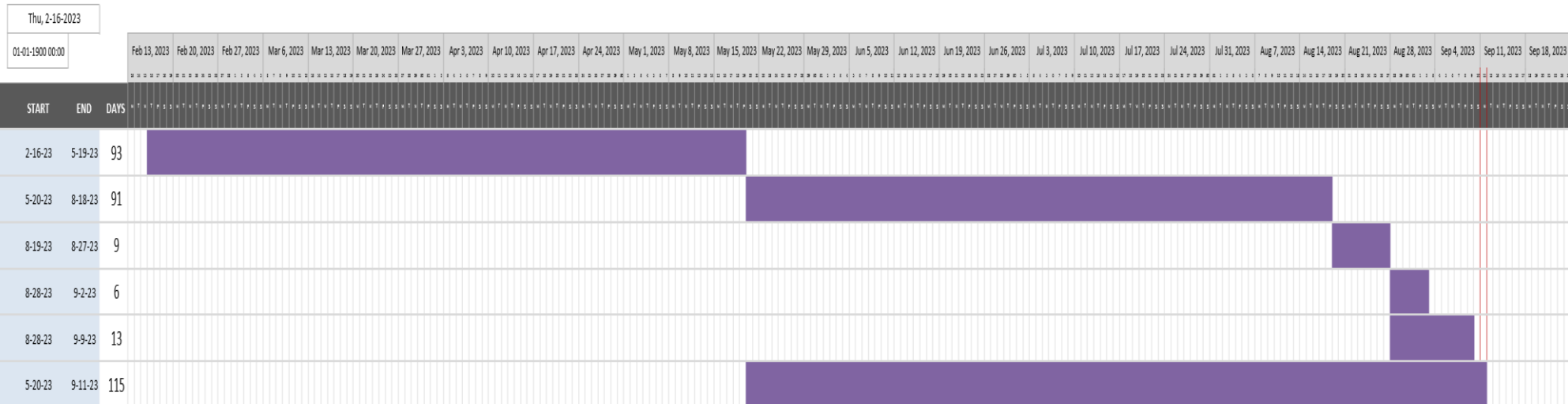


*Figure 3: Updated Gantt Chart*

Figure 3 represents the realistic timeline for each task. Consistent with the proposed Gantt Chart, the literature review was completed within 3 months. During the designing phase, several challenges were faced such as dealing with leakages and deformed casts. To overcome these problems and create a robust device, various design changes were implemented. The excess time in the designing phase, impacted the time allocated for the other parts of the project. However, the objectives laid out for this project was successfully completed within given time frame.

## Related Work

Haptic feedback systems, as discussed in the previous section, are broadly divided into Kinesthetic or Cutaneous feedback systems. Vibration motors, Piezoelectric actuators and Pneumatic systems are the top preference for developing a Cutaneous feedback system. MR Fluids and haptic systems are rarely explored. They are usually used in damping and providing variable resistance against impact load. A niche number of systems exist, however focusing on providing Kinesthetic feedback. Y.J Nam et.al [5] has developed a novel haptic glove which uses MR fluid-based actuator to provide passive actuation. A novel tendon mechanism is used, which is capable of transmission of position and force between the finger tips and the actuator. Scott H et.al [6] developed a similar force feedback glove, which used MR Fluids to generate resistive force. A piston is attached to an exoskeleton, which covers the length of the finger, through a wire providing resistance to the motion of the finger. Gaoyu Liu et.al [7] talks about the medical application of MR Fluids. According to the article, MR Fluids can be used in numerous medical application such as Prosthetics, Exoskeleton, orthosis, haptic master, and tactile displays. The author suggests the use of MR dampers and brakes to provide variable damping and resistive forces. Technologies such as Haptic master is suggested for teleoperation which could provide realistic force sensation experienced by slave robot. MR Fluids are also used passively to provide Kinesthetic haptic feedback during endovascular tele-operation. Yu Song et.al [8], developed an MR Fluid based haptic feedback system, to generate a change in the fluids viscosity when collision is detected by the slave robot during catheter insertion. The catheter goes through the MR Fluid tube which is placed in between two magnetic poles. The author describes the sensation similar to inserting a rigid cylindrical tube into a sticky clay [8]. MR Fluid based pulse generation devices have been used to simulate human pulse for various ages. A device by Miranda Eatson et.al [9] generates range of human radial pulse by using MR fluids to expand or contact a silicone tube. The tube manipulation region is in contact with a plunger which displaces when the fluid is actuated using a magnetic field generating a pulse. A cam system is used to generate baseline pulse and is evaluated against displacement produced using MR Fluids. A system by Jeong-Hoi Koo et.al [10], which has a similar setup as [9], have used MR fluids to generate variable human radial pulse profiles. Instead of using a Plunger, this system alters the flow rate of the MR Fluid. Altering the electromagnet's intensity and actuation frequency, the author was able to create a 30% flow rate drop and a variable flow rate of 31 to 100 mmHg.

A combination of Kinesthetic feedback with cutaneous feedback have been explored by number of researchers. Such systems are complex to design however provide promising results in teleoperation tasks. A CyberGrasp ® is integrated with a custom motor driven tactile feedback device and a vibrotactile feedback system to sense and display local tactile activities by Jenna L. Graham et.al [11]. The aim here was to provide Kinesthetic, vibratory, and tactile to help understand the environment better during teleoperation [11]. Rebecca M Pierce et.al [12] controlled a Willow Garage PR2 humanoid robot's parallel-jaw gripper using an ingenious hand-wearable haptic-device. This system is capable of producing Kinesthetic and cutaneous feedback. An optical encoder on a geared DC motor is used to generate constant torque on the user's finger providing force feedback. Two voice-coils actuators, placed behind the distal Phalanges of the thumb and the index fingers are used to generate pressure force during gripping an object and removal of contact [12].

Cutaneous feedback systems can generate normal or lateral forces on human skin. They are relatively easier to generate, however, display low magnitude of forces. Devices based on pressure or normal forces are common, however, it is difficult to design a system generating normal and lateral forces. Samuel et.al [13] have used delta mechanism to develop a skin deformation device that generates lateral forces and change in normal forces on the finger. The device uses two DC motors and gearboxes to move a soft tacter. The device is evaluated using two virtual environment tests, performed by 26 users, a palpation test and a friction rendering experiment. The results provided for evaluation ensures the robustness of the system, however, the mechanism for producing forces is complex and may introduce slack on the joints. The motor and the pulley mechanism present on top of the lateral support [13] will make the device uncomfortable to use after a while. A belt and pulley arrangement has been developed by S.H Atapattu et.al [14] to generate normal and lateral forces through pressure and vibration. This is a wearable device which runs on six micro gear motors enclosed on a 3D printed case. Having three belts enables this device to generate variable pressure and vibration profiles on different areas of the finger. Such device will be able to generate forces much efficiently when compared to systems like [13]. A haptic thimble for surface exploration was developed by Massimiliano Gabardi et.al [15] which has a novel gear arrangement and a voice coil to produce 2 rotation and one translation forces. The rotation forces are aimed at producing surface curvature and orientation. The translation motion is for generating normal forces. A similar haptic thimble was developed by Hwan kim et.al [16] for rendering direct-touch feedback for virtual touch screen interaction. This device provides normal, vibration and lateral forces on the finger tips.

A spring and lever arrangement attached to a cap in contact with the index finger, slides laterally to provide shearing and pressure. PZT chips have been considered for cutaneous feedback systems [17]. Using PWM, Minglu Zhu et.al [17] used a PZT chip to generate feedback for their smart glove. The device can detect normal and shear forces using triboelectric based sensors. Piezoelectric actuators can be used to generate a lateral sensation, however, might not be sufficient for generating normal forces. A pneumatic based system was developed by Antonia Tzemanaki et.al [18] for determining surface stiffness properties on a virtual environment. A rack and pinion mechanism were used with an IMU sensor to adjust a polylactic acid filament, 3D printed platform. This system generates indentation on the finger tips using compressed air. Vibrotactile actuators are like PZT chips but are actuated using a miniature DC motor with an offset mass [19]. Such actuators have been used to generate pressure forces and simulate stiffness, however cannot provide any lateral sensation.

## Methodology

### Magnetorheological Fluid

Magnetorheological fluids (MR Fluids) are smart materials exhibit fast and reversible transition from solid to liquid under the effect of magnetism. The conversion is usually within milliseconds. These fluids are two-phased and contain micron-sized highly magnetizable solid particles suspended in a non-magnetizable carrier fluid. Additives are added to stop sedimentation, accumulation and provide extra lubrication. Common additives used include thixotropic agents, surfactants, and polymers [20].

MR fluids under magnetism produce MR effect. In presence of magnetic field, the magnetic particle attracts each other, along the field line, which forms anisometric aggregates. The resultant formation exhibits large yield stress [20] and form columnar structures in the direction of applied magnetic field [21]. On loosing magnetism, the fluid possesses low viscosity and behaves similar to Newtonian Fluids [20]. On the other hand, colloidal ferrofluids do not inherit particle structuring or resist flow under magnetic field. Instead, the magnetic force causes the entire fluid to be fixed in the region of high magnetic field which causes minimal or no increase in rheological properties [22].

Generally, MR fluids inherit large magnetization saturation and lower coercivity. It is also operational over a wide temperature range, and stable against settling, irreversible flocculation, chemical degradation, oxidation [20]. As these fluids have unique controllable rheological

properties, they are mostly used to control shock, and vibration. Such devices will have very few moving parts and can provide variable damping controlled by magnetism. Hence, MR fluid devices experience less wear and long-life expectancy [22]. The MR Fluid used for this thesis is developed by Lord corporation and is called as MRF-132DG. Table 1 provides the various technical data for the MR Fluid used in this project. According to Osama et.al [22] iron alloy particles are used instead of traditional iron particles which produce higher yield stresses than other kind of MR fluids.

Table 1: Properties of MRF-132DG

Parameter	Value
<b>Appearance</b>	Dark Gray Liquid
<b>Viscosity, Pa-s @ 40°C</b>	$0.112 \pm 0.02$
<b>Density (g/cm3)</b>	2.95-3.15
<b>Solids Content by Weight, %</b>	80.98
<b>Flash Point, °C</b>	>150
<b>Operating Temperature, °C</b>	-40 to +130

MR fluids usually consist of three major components: ferromagnetic particles, carrier fluid and stabilizers. Ferromagnetic fluids are spherical shaped particles with diameter ranging from 1-10 micro meter and have a density of  $7-8\text{g}/\text{cm}^3$  [22]. Carbonyl iron magneto-soft powder, which has high magnetic permeability is a common magnetizable particle used for MR fluids. The carrier fluid acts as continuous insulating medium [22]. Osama et.al advices the appropriate viscosity range for carrier fluids to be  $0.01-1.0\text{ Ns}/\text{m}^2$  at  $40^\circ\text{C}$  [22].

Image produced from [22].

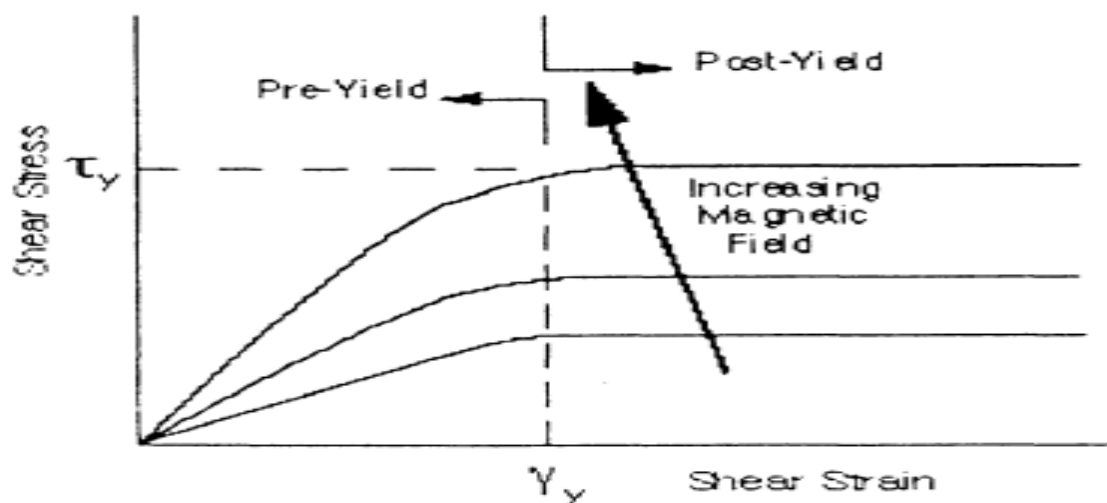


Figure 4: pre-Yielding and post-yielding region of MR Fluids

## Characteristics of MR Fluids

MR Fluids behaves like Newtonian fluids when the suspended particles are unrestricted and not influenced by an external field. This behaviour can be explained by the Hagen-Poiseuille law. However, under magnetic influence, each particle is converted into a dipole which enables them to form a chain with boundary elements. This semi-solid will resist shear rate up to a certain extent, exceeding which will break down the chain and enable the fluid to flow. This behaviour is usually explained by Bingham plastic model or Herschel-Bulkley Model. Osama et.al [22] explains the overall behaviour of MR Fluids with pre yielding and post yielding zones. The figure 4 presents the corresponding regions.

### Pre Yielding behaviour of MR Fluids

MR fluids, pre yielding, behaves like Newtonian fluids. Such behaviour can be explained by the Hagen Poiseuille equation. According to Poiseuille's law the flow rate depends on fluid's viscosity, the pipe's length, and the pressure difference between the point of measurement [23]. This equation assumes the fluid to be incompressible, Newtonian, non-heat-conducting, and the flow rate to be laminar [24]. Hagen- Poiseuille law indicates the velocity profile of such fluids to be parabolic [24]. This can be represented using the following formula [23]:

$$Q = \frac{\pi r^4 \Delta P}{8\eta L} \quad (1)$$

In the above formula,

$Q$  = Volume flow rate ( $m^3/s$ )

$r^4$  = the inner radius of a pipe (m)

$\Delta P$  = Pressure difference between the cylinder ends (Pa)

$\eta$  = Dynamic viscosity of the fluid (Pa s)

$L$  = The length of the pipe (m)

To study the Newtonian behaviour of the fluid, an experiment was conducted to determine the fluid viscosity under the absence of magnetic field. A circular pipe was connected to a pump such that the fluid can pass from one section the pipe to another. A peristaltic pump was used for this experiment. A digital manometer was used measure the pressure at the inlet and the outlet of the pipe. The experimental setup is shown in the figures 5 and 6.

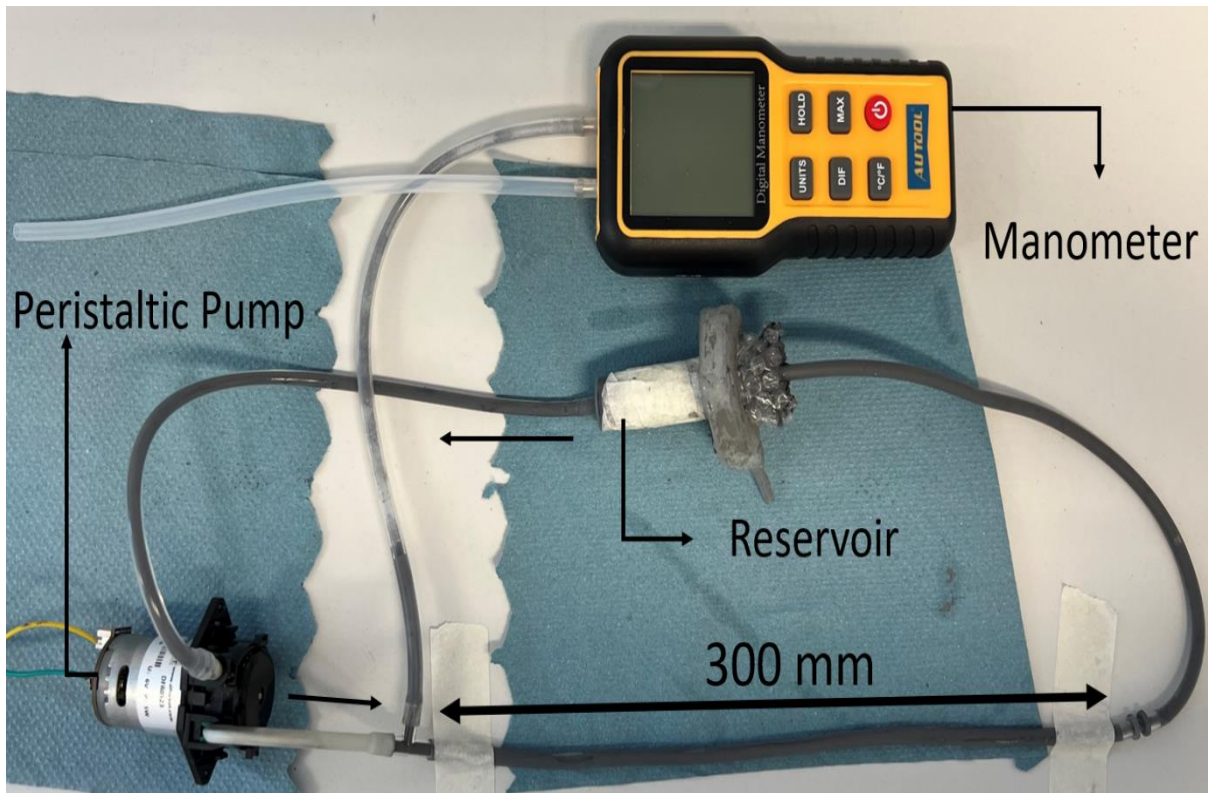


Figure 5: Setup to determine the Inlet Pressure

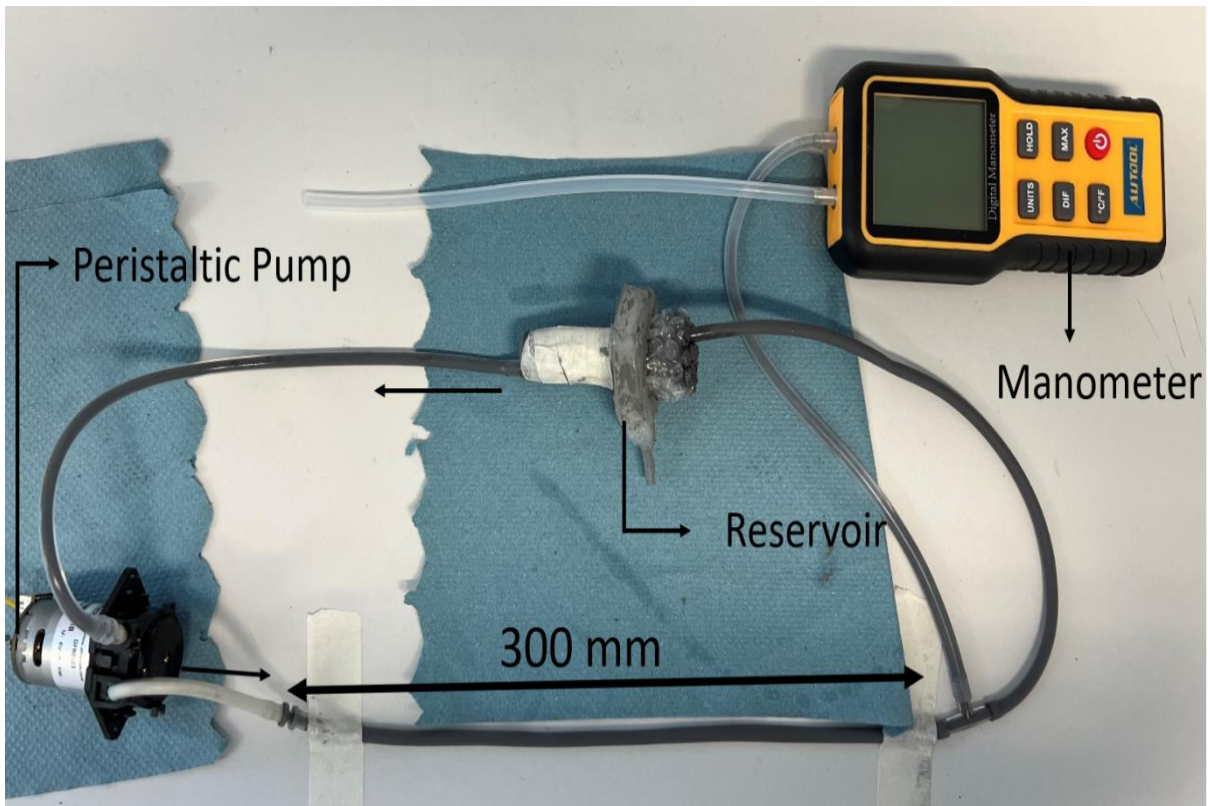


Figure 6: Setup to determine the Outlet Pressure

The figures above represent the experimental setup to measure the inlet and outlet pressure of a pipe of length 300 mm. The pipe is taped at both ends to ensure it is straight and has a uniform cross section. This will ensure that the flow across the pipe will be laminar. To determine the

dynamic viscosity of the MR Fluid, equation-1 will be used. On rearranging the variables of equation 1, we have:

$$\eta = \frac{\pi r^4 \Delta P}{8QL} \text{ Pa s} \quad (2)$$

The inlet pressure of the pipe, using the manometer, was measured to be in the range of 10000 Pa to 9000 Pa. Table 2 represents the values obtained from the manometer.

*Table 2: Inlet and Outlet Pressure values*

	Inlet (Pa)	Outlet (Pa)
<b>Observation 1</b>	10140	1817
<b>Observation 2</b>	9055	1999
<b>Observation 3</b>	9301	2354

To get an accurate measurement, three values from the manometer were recorded and was averaged. A similar approach was taken for measuring the outlet pressure. Hence the various parameters of equation-1 are:

$$P_{inlet} = 9498.66 \text{ Pa}$$

$$P_{outlet} = 2055.66 \text{ Pa}$$

$$\Delta P = 7442.99$$

$$Q = 85 \text{ ml/min} = 0.085 \times 10^{-6} m^3/s$$

$$L = 300\text{mm} = 0.3\text{m}$$

$$r^4 = 4\text{mm} = 0.004 \text{ m}$$

Substituting in equation 2, we have:

$$\eta = \frac{\pi \times (0.004)^4 \times 7442.99}{8 \times 0.085 \times 10^{-6} \times 0.3} \\ \eta = 0.4743 \text{ Pa-s at } 23.5^\circ\text{C} \quad (3)$$

According to the data sheet [25] provided, the viscosity value of the fluid at 40°C was determined to be  $0.112 \pm 0.02$  Pa-s. The dynamic viscosity of the fluid, using equation 3 is 0.4743 Pa-s. According to [26], the dynamic viscosity of liquids decreases as temperature increases. This fact is consistent with the calculations obtained in equation 3. The values

provided by the datasheet was determined at 40°C. However, the values obtained from the manometer was at an ambient temperature of 23.5°C.

### Post Yielding behaviour of MR Fluids

According to Xiaojie Wang et.al [27], the flow of ER and MR Fluids through a circular pipe with uniform cross section, can be described using the Herschel-Bulkley equation. The equation is given by [27]:

$$\tau_{rz} = \tau_y + k \left| \frac{du}{dr} \right|^n \text{ for } |\tau_{rz}| \geq \tau_y \quad (4)$$

$$\frac{du}{dr} = 0 \text{ for } |\tau_{rz}| \leq \tau_y \quad (5)$$

Where,

$\tau_{rz}$  = Shear Stress

$\frac{du}{dr}$  = Shear rate

$\tau_y$  = fluid's yield stress

k = Fluid Consistency Index

n = Fluid Behaviour Index

Image printed from [28]

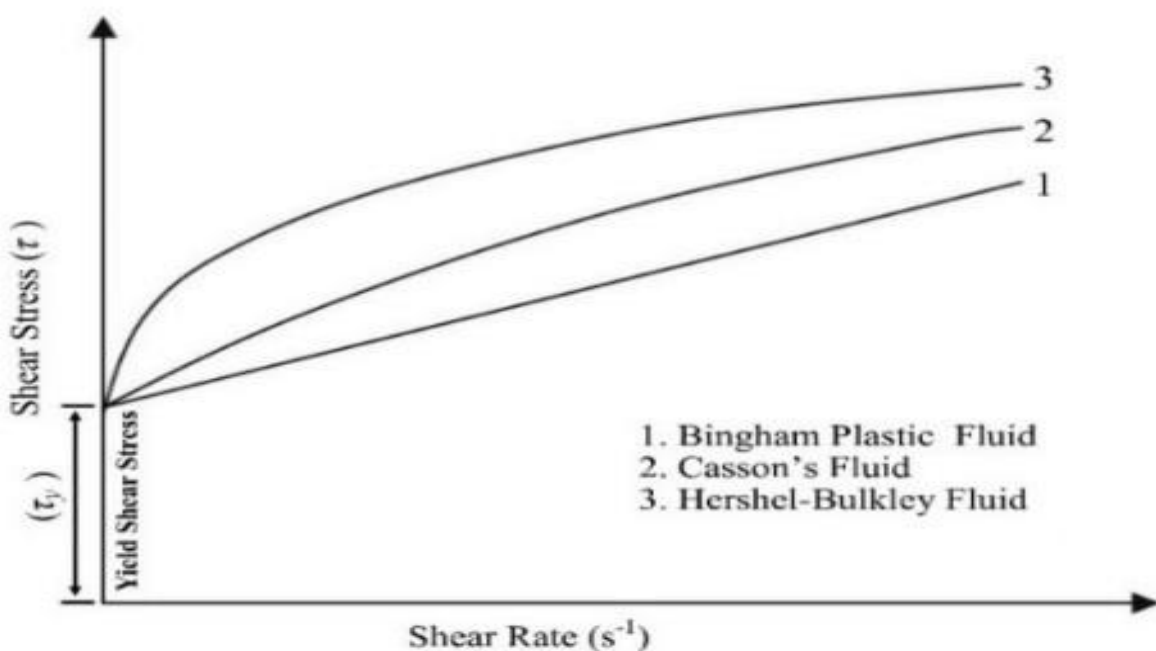


Figure 7: Typical Behaviour of Non-Newtonian Fluids

The figure above represents the shear rate vs Shear Stress graph for three models; Bingham Plastic model (1), Casson's Fluid Model (2) and Hershel-Bulkley Fluid (3). According to equation 4, shear stress is dependent on the yield stress, the fluid consistency index, the fluid behaviour index, and shear rate. The fluid consistency index ( $K$ ) is related to the viscosity of the fluid. The fluid behaviour index( $n$ ), determines the fluid to be Newtonian or non-Newtonian. If  $N= 1$ , the fluid is categorized Newtonian,  $N<1$  is termed as pseudoplastic and  $N>1$  is Dilatant [29]. However, the nature of relationship is non-linear. The above figure provides an idea of the typical behaviour of non-Newtonian fluids. According to figure 7, such fluid possesses a yielding stress, which will resist the flow, making the flow rate as zero. However, once the threshold for the yield stress is surpassed, the fluid experiences shearing. The sharing rate and the corresponding stress can be linear or non-linear in nature.

A high  $K$  value will correspond to high resistance to flow which will increase the viscosity of the fluid. A high viscosity value will increase the shear stress of the fluid which will decrease the flow rate. In the non-Newtonian phase, under high viscosity and high shear stress, the fluid will exert a normal force on the walls of the enclosing surface, as seen in [9,10].

A cutaneous device which can generate normal as well as lateral forces are difficult to generate. Use of complex mechanical links, such as delta mechanism [13], can generate higher magnitude of lateral and pressure force but can be heavy for real life applications. Also, the control mechanism is complex. PZT, vibrotactile actuators and pneumatics are easy to implement but are mostly mapped for either pressure or shear forces [17,18,19]. Servo based device [1,3,2] can be used to develop greater than 1 DOF cutaneous cues but can be uncomfortable to wear. The plastic and metals parts can cause pseudo vibrations causing false feedback and can get relatively heavy after using for certain time period. MR Fluids, due to their high and controllable shearing properties, are mostly used as damping and resistive device to develop Kinesthetic feedback devices [5,6]. Commercial MR devices for medical applications have also been explored but as dampers, brakes, and clutches [7] which categorize as resistive devices. However, MR Fluids have been rarely been used for development of cutaneous devices. Systems developed by [9] and [10] are evidence that the MR effect can be used to generate pressure and normal forces.

Keeping the above shortcomings in mind, this project attempts to create a cutaneous haptic device which is light, easy to operate and produces normal as well as lateral forces. This device uses the controllable and shearing properties of MR Fluids to generate pressure and lateral

forces on the index finger through displacement of the device surrounding it. The actuation is provided using an electromagnet which sits external to the haptic device. The wearable device is silicone rubber based and flexible in nature which can accommodate multiple size fingers. The system can generate variable frequency and intensity of pressure and lateral forces.

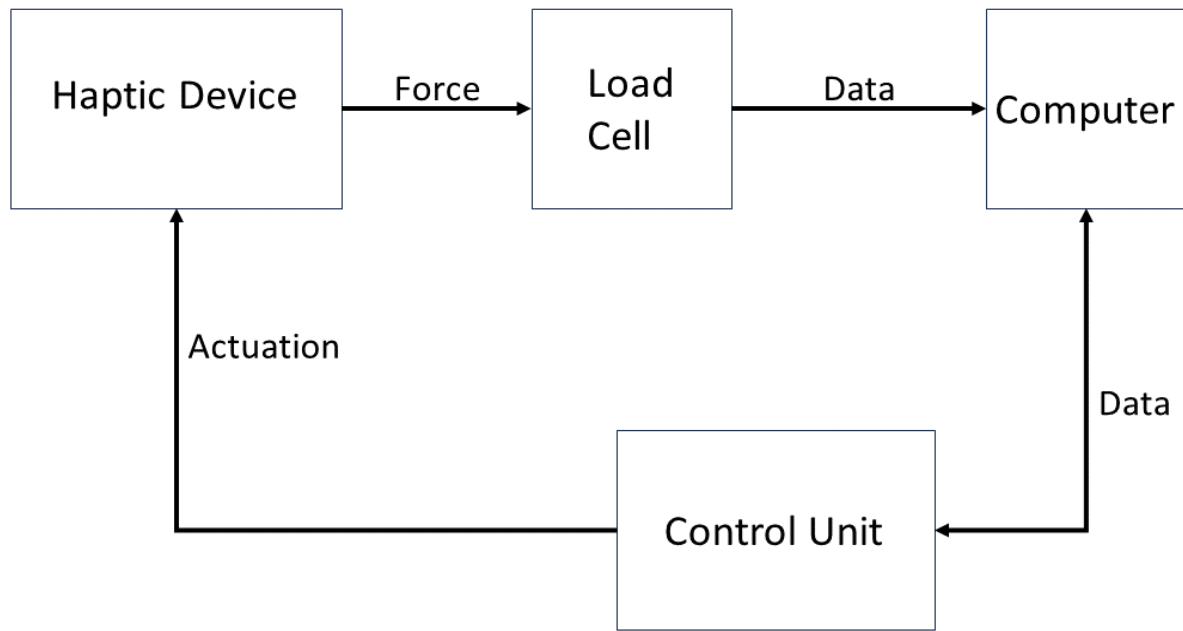


*Figure 8: System Overview*

The figure above represents the various components involved in controlling and actuating the haptic device. The complete system consists of an ingenious haptic device which is actuated based on signals from the control unit. The control unit communicates to a computer using a microcontroller. A load cell sensor is used to capture the forces produced by the haptic device. The data from the load cell sensor is interpreted by an electronics box which communicates to the computer using USB protocol.

## Design of the wearable haptic device

The wearable haptic device consists of two layered rubber silicon which are connected to each other and have hollow channels between them. The hollow channels are intended to allow the MR Fluid flow from one end to the other. Each layer is approximately 1mm thick. The diameter of each channel, assuming them to be cylindrical in nature, is approximately 4mm. One side of the bottom layer is in contact with the index finger. This contact will transfer force from the fluid to the finger which is received by the tactile receptors located the human skin [1]. The

initial approach for developing this device was to cast the top layer and the bottom layer separately. A 3D printed Mold was designed using the Fusion 360® software. The images below represent the cross section of the inner and the outer layer.

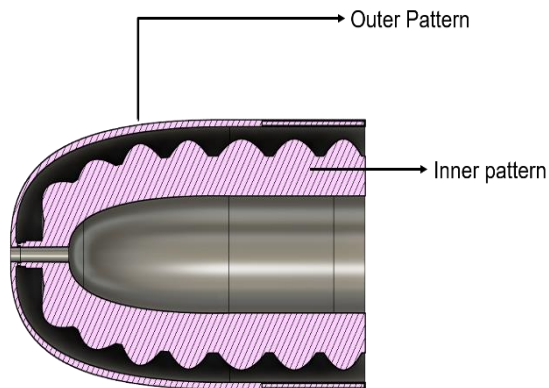


*Figure 9: Outer layer Mold*

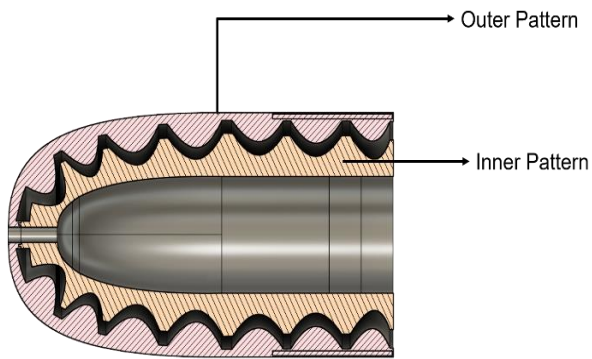


*Figure 10: Inner Layer Mold*

The above figures represent the various parts of the 3D printed Mold. The Molds consisted of three removable parts, the inner pattern, the top half of the outer pattern and the bottom half of the outer pattern. The indentation on the patterns casts the hollow channels between the skins. The casting process was done using Ecoflex ® 00-30. The product contains two parts of liquid, marked as “Part A” and “Part B.” In order to develop a mixture for casting, equal parts of part A and part B is mixed thoroughly, eliminating any air bubbles from the mixture.

After casting the first iteration of the skins, it was observed the cast was subjected to certain deformities and air bubbles. The air bubbles made the skins imperfect to use compromising their structural integrity. It was also observed that the layers will be difficult to bind together due to the complex curvature. The images below show the results from the first iteration.

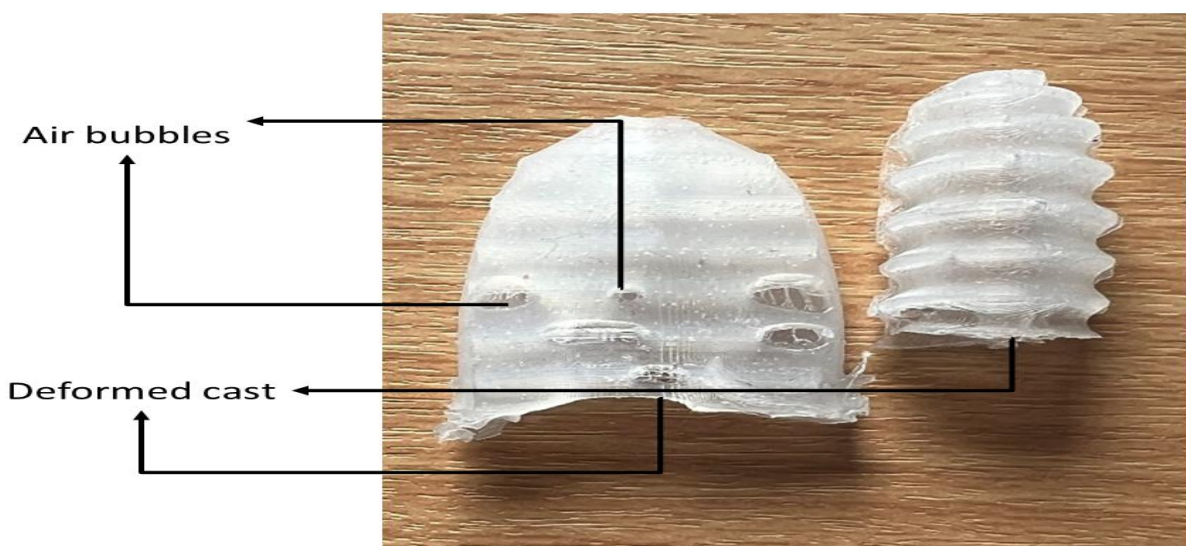


*Figure 11: Cast from the first Iteration*

Considering the above complications, a new approach was taken. In the new iteration, the top layer and the bottom layer was casted together, omitting the need for binding the layers post the casting. A new mould was designed which had a base, two removable walls and multiple cylindrical bars for creating the hollow channels. Figure 13 and 14 represents the improved Mold design.

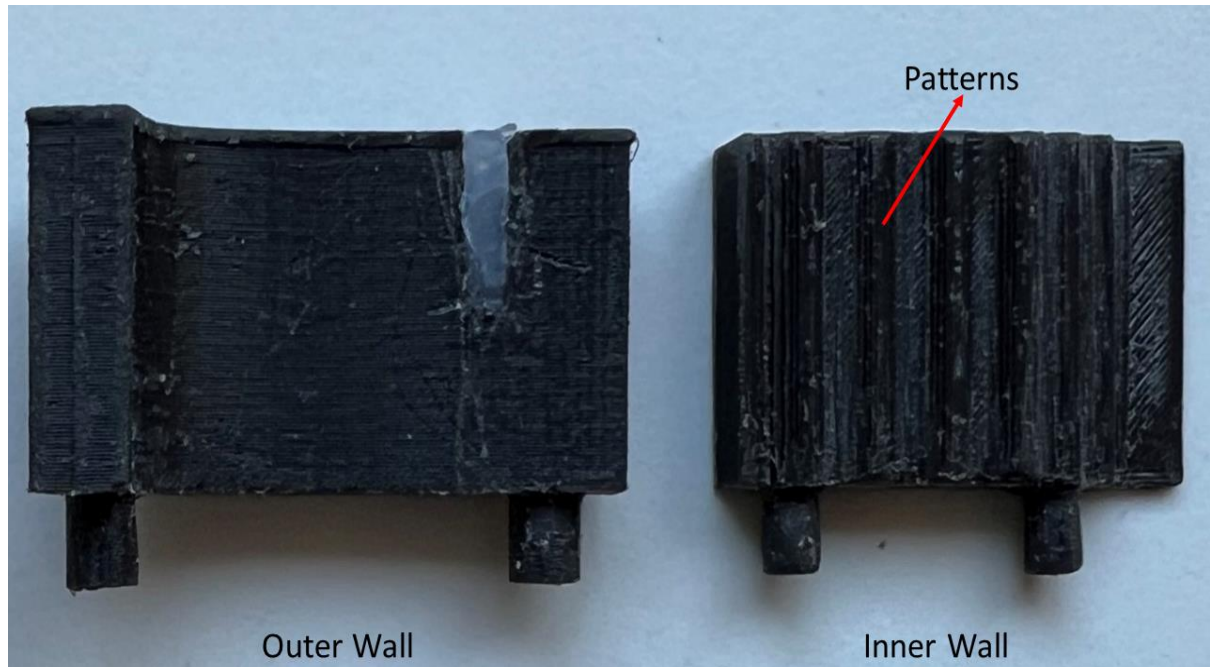


Figure 12: The Outer and Inner wall patterns of the Mold

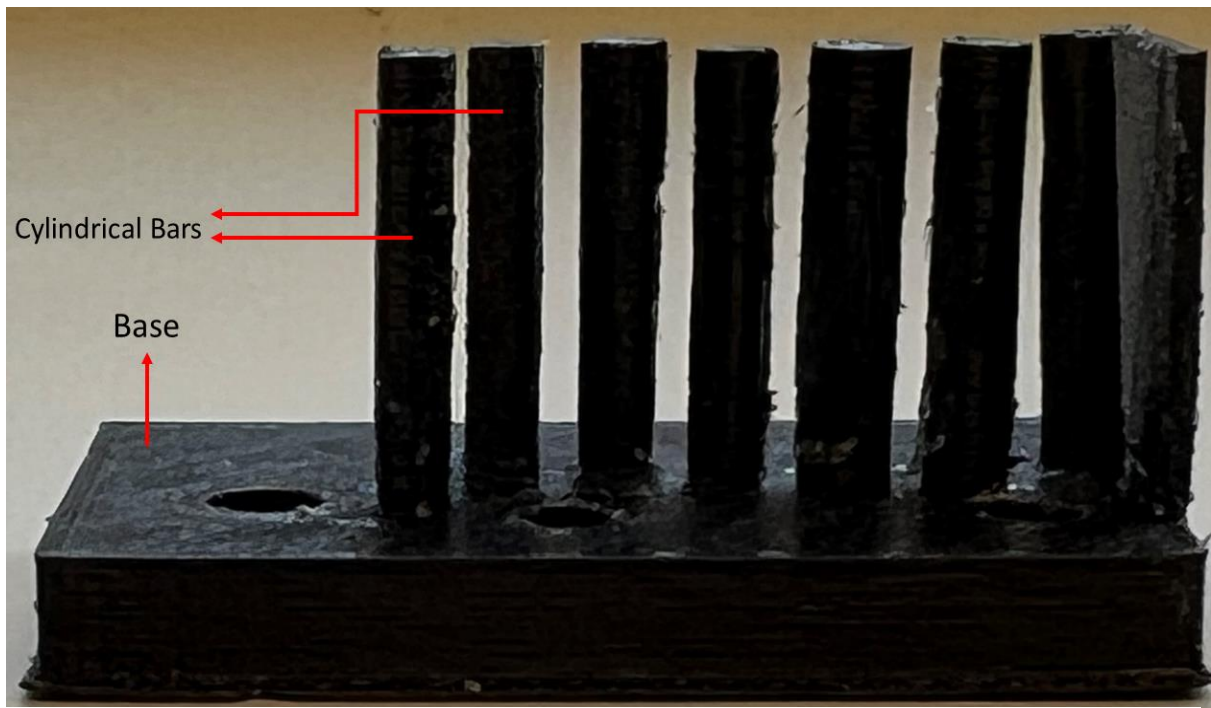
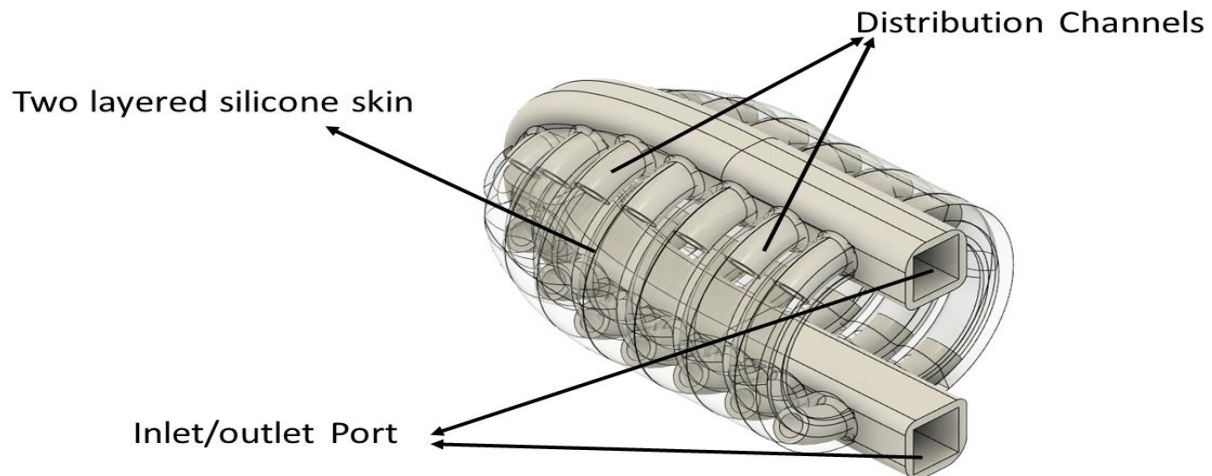


Figure 13: Mold For generating Internal Channels

Two set of skins were casted which was connected to a 3D printed pipe. The pipe had distribution channels corresponding to the hollow channels which was intended to introduce MR fluid into the silicone rubber. The pipe is hollow along its length which serves as the inlet or the outlet port of the haptic device. The complete assembly contains two set of double layered silicone rubber connected to two 3D printed pipes. The figure below shows the 3D model of the final assembly and the structure of the 3D printed pipe.



*Figure 14: 3D Model of the Haptic Device*

The total length of the haptic device is around 35mm. This front side of the device has a similar curvature to human fingers. This curvature ensures a comfortable and natural fit on the user's finger. The design also generates strong contact between the inner side of the silicon rubber and the human skin. The 3D printed pipe has flat side which ensures minimal pressure on the

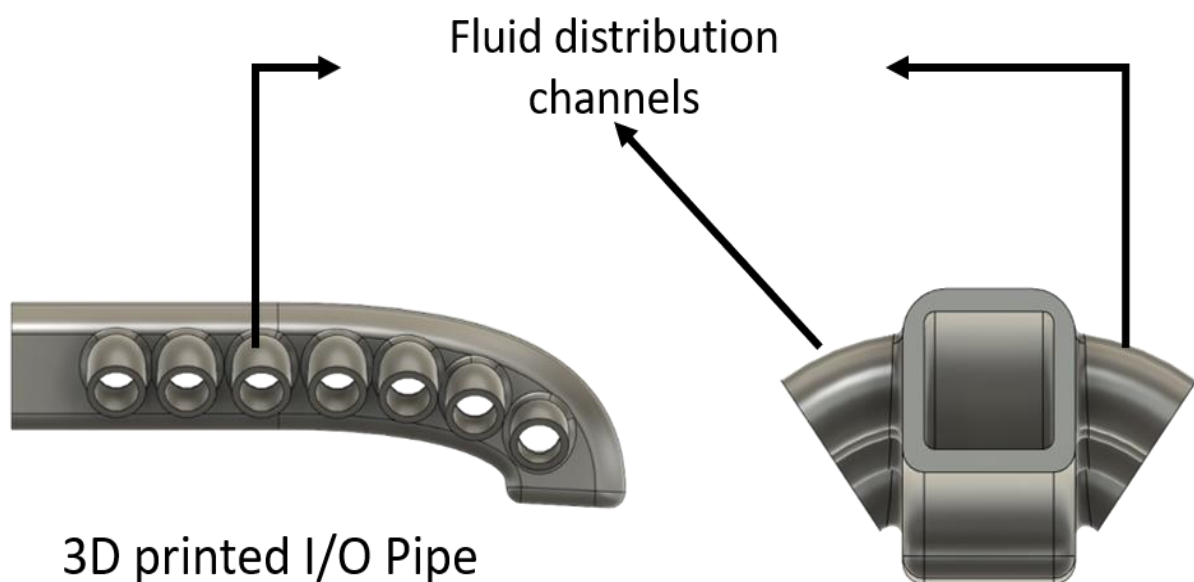


*Figure 15: 3D model of the Inlet Outlet Pipe*

user's finger. This will help use this device for prolonged hours. The flexible nature of the silicone rubber also makes the device capable of handling variation in pressure.

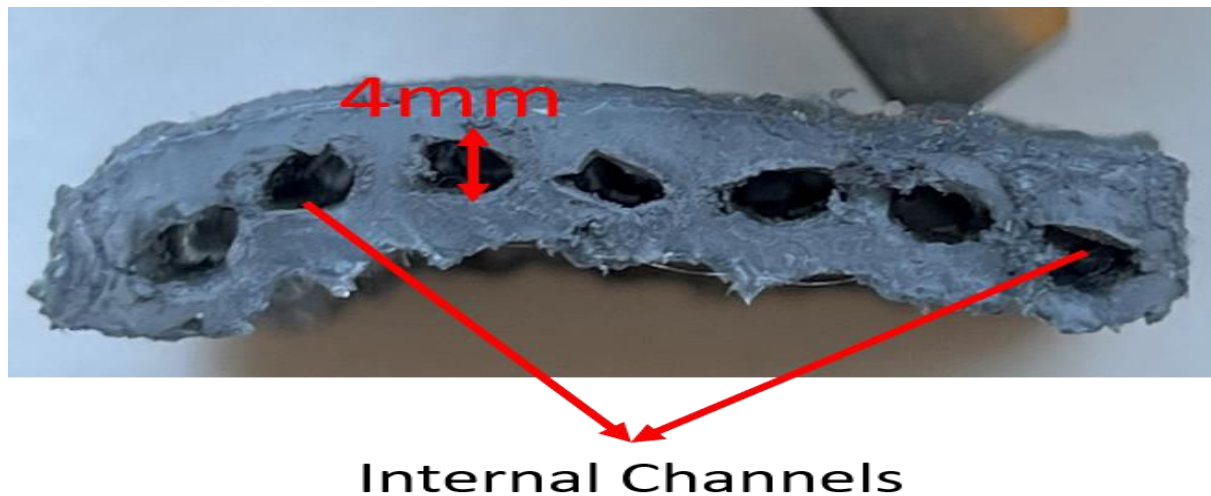


Figure 16: Cross Section of the two layered skin



Figure 17: The Top and the Bottom Skin

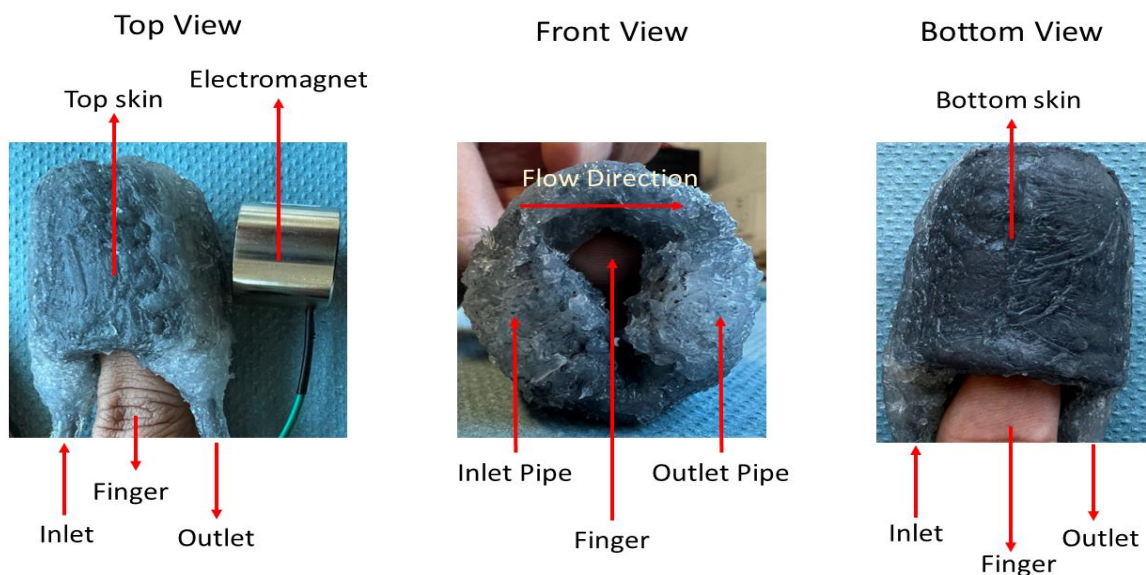


Figure 18: The Top, Bottom, and the Front view of the Haptic Device

The silicone rubber skins have 7 hollow channels and are approximately 4mm in diameter. The total thickness of each cast is approximately 6mm. The length of the top part and bottom part is 40mm and 60mm respectively. Figure 17, 18 and 19 shows the casted parts and the final assembly

## System Overview and circuit diagram

This section talks about the various electrical components involved and the overall circuit diagram in this project and their specification. The exact working of the system is explained.

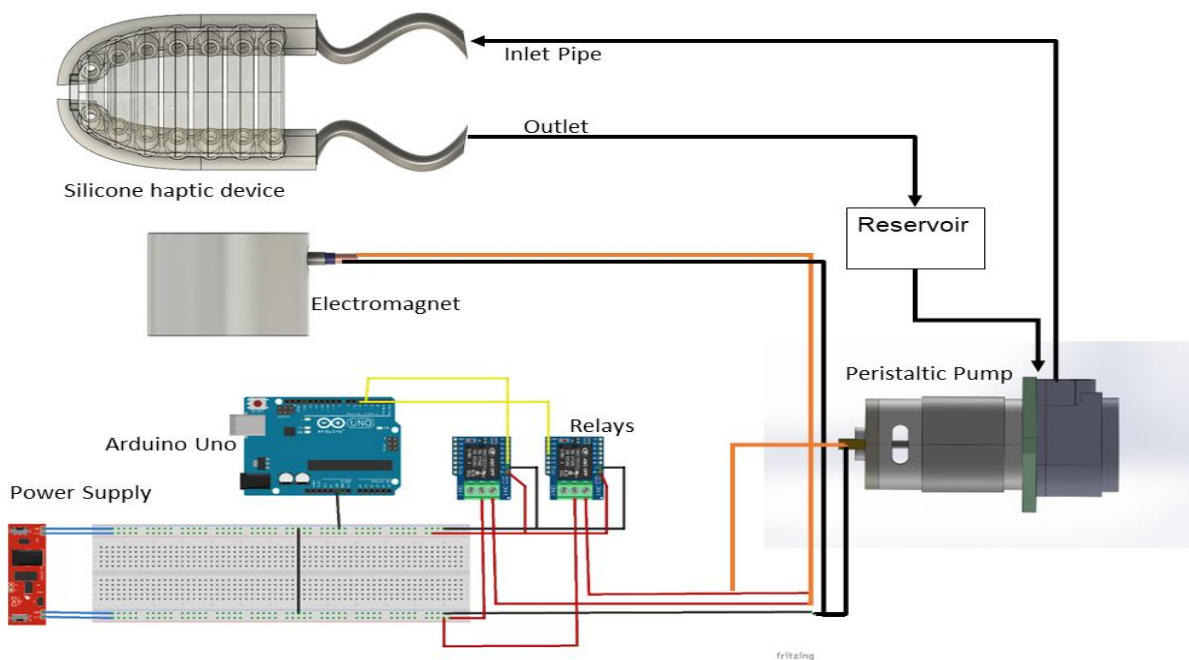


Figure 19: The circuit diagram with the Haptic Device

The figure above demonstrates the overall system. The system consists of an Arduino Uno, a 2-channel relay module, a peristaltic pump, and an electromagnet. The relay module uses a 12v operating voltage and uses a 5V or 3.3V signal for switching. The module contains a normally open port, which acts an open switch, a common port and, a normally closed port, which will close the circuit when the module is not signalled. The PCB is manufactured by Gravitech [30] and is rated for 125V 8A DC. The operating time is 10ms.

The peristaltic pump is a positive displacement pump, which has a DC motor driving three rollers. These rollers are preset in a closed case and rotates on flexible pipe laterally. The lateral movement squeezes the tube creates a pumping effect [31]. The pump used for this project is a digital peristaltic pump by DFRobot [31]. A PPM motor driver is integrated with the pump. As the rollers are not in direct contact with the fluid, makes it ideal for applications such as medical and pharmaceuticals. The efficiency of MR fluids depends on the quality of fluid. A geared

pump might contaminate fluids during wearing and tearing of the gears. Considering all the factors discussed, a peristaltic pump is the ideal choice for this project. The pump works on 5V DC and consumes 2W of power.

The electromagnet consumes 5V and 0.5A of current. It takes 2.5 W of power and provides a lifting force of 50N. The electromagnet is connected to the common and the normally open ports of the relay module on the first channel. The second channel is connected to the peristaltic pump using the common and the normally open port.

The outlet of the pump is connected to the inlet port of the haptic device. The outlet of the haptic device is linked to a reservoir which holds the fluid. The reservoir is joined to the inlet port of the pump. This system enables the MR Fluid to flow from the reservoir, through the pump, into the haptic device and back to the reservoir.

## Implementation

As the electromagnet is magnetized near the haptic device, the ferromagnetic particles form a chain structure. As shown in the fig 21, the cross-section of the skin can be approximated to a cylindrical pipe of inner radius 4mm. If the pump is in the OFF state, i.e., the fluid is stationary, and no other force is present to surpass the yield stress caused by the MR effect, the semi-solid fluid will exert normal forces on the inner wall of the haptic device causing a displacement. The figure 21 demonstrates this process. The above stated concept has been used for developing artificial Human radial pulse generating systems [9,10]. The apparatus developed by [9], used MR Fluids in silicone tube to displace a plunger placed on the walls of the tube, through MR effect. According to [9], when MR fluid is actuated using an electromagnet, the silicone tube

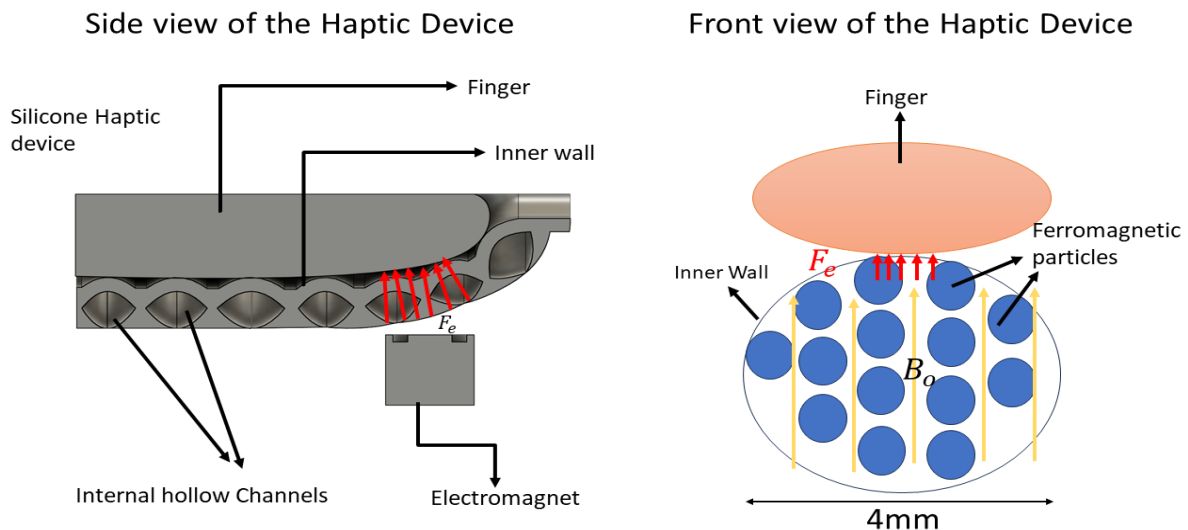


Figure 20: Normal Force Generation

expands as the fluid transforms from liquid to semi-solid and, the plunger displaces with a corresponding amount. The displacement of the plunger is controlled by the intensity and frequency of activation of the electromagnet [9]. The system by [10] generates passive pulses by altering the flowrate and the pressure of the MR Fluid. Electromagnets are used to regulate the fluid's apparent viscosity which generates pulse wave patterns [10].

In figure 21, let  $B_0$  be the magnetic field created by the electromagnet. The yellow lines represent the lines of the magnetic field. The ferromagnetic particles present in the MR Fluid aligns in the direction of the magnetic field and creates a chain formation. This chain structure exerts a force  $F_e$  on the Glabrous skin which are sensed by the mechanoreceptors present under the human skin.

This haptic device generates pulse on the index finger when an electromagnet is magnetized around it. As the activation area of the electromagnet is limited, the forces developed against the wall will quickly disperse. Hence to generate continuous forces, the frequency of activation of the electromagnet is varied.

If the activation frequency is as little as 5Hz, and the fluid experiences a pressure drop by the Pump, lateral forces are generated tangential to the curvature of the fingers. The figure below, represents these forces:

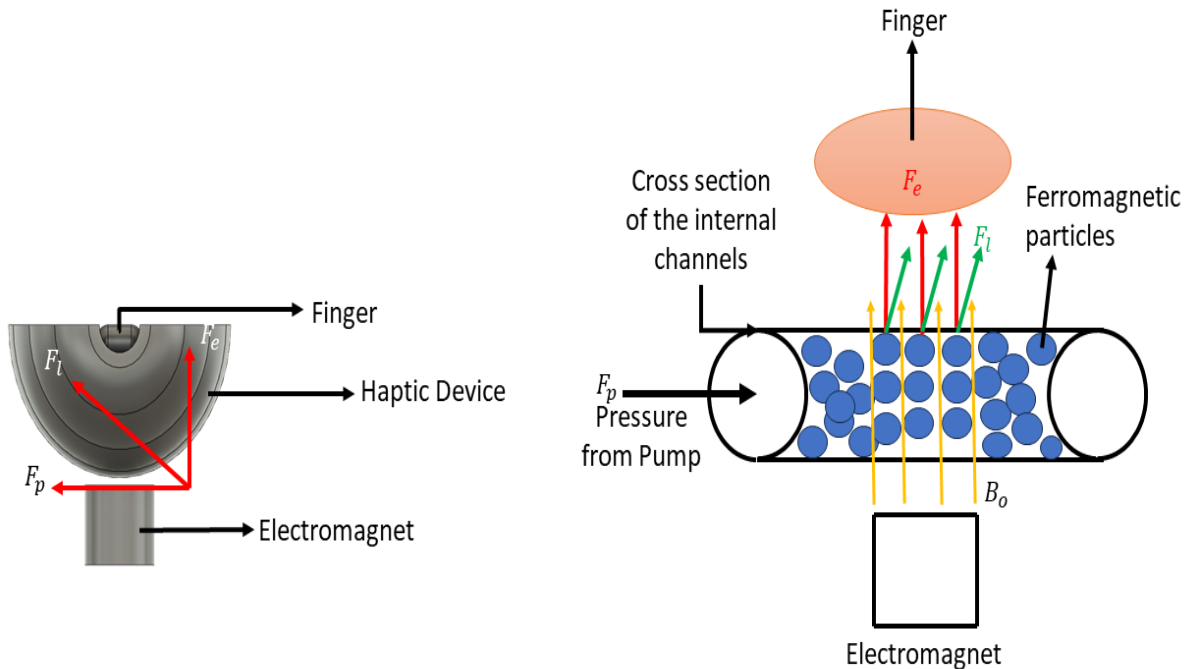


Figure 21: Shear Force Generation

Assuming the forces created by the pump on the fluid as  $F_p$  and force exerted by the fluid due to the MR effect as  $F_e$ . By triangle law of forces, there must be a force which will be generated between  $F_p$  and  $F_e$ . Let us represent this force by  $F_l$ .  $F_l$  is responsible for creating a force tangentially on the fingers. However, as the pressure force on the finger is not constant, the lateral forces generated will vary in magnitude and will be cyclic.

## Experiments and Results

To evaluate the haptic feedback system, three sets of experiments were conducted. The first experiment determined the magnitude of normal forces with varying activation frequency of the electromagnet. Extending the approach, the lateral forces generated by the haptic system was determined in the second test. The third test was done with a Franka Emika gripper.

### Evaluation of Normal forces

For determining the magnitude of the normal forces and the responsiveness of the system, a 6-axis load cell sensor was used. The load sensor is manufactured by Resense and is capable of sensing force in 3 axis, X, Y and Z of magnitude up to 125N and moment in same axis up to 2.25Nm. The figures below show the experimental setup:

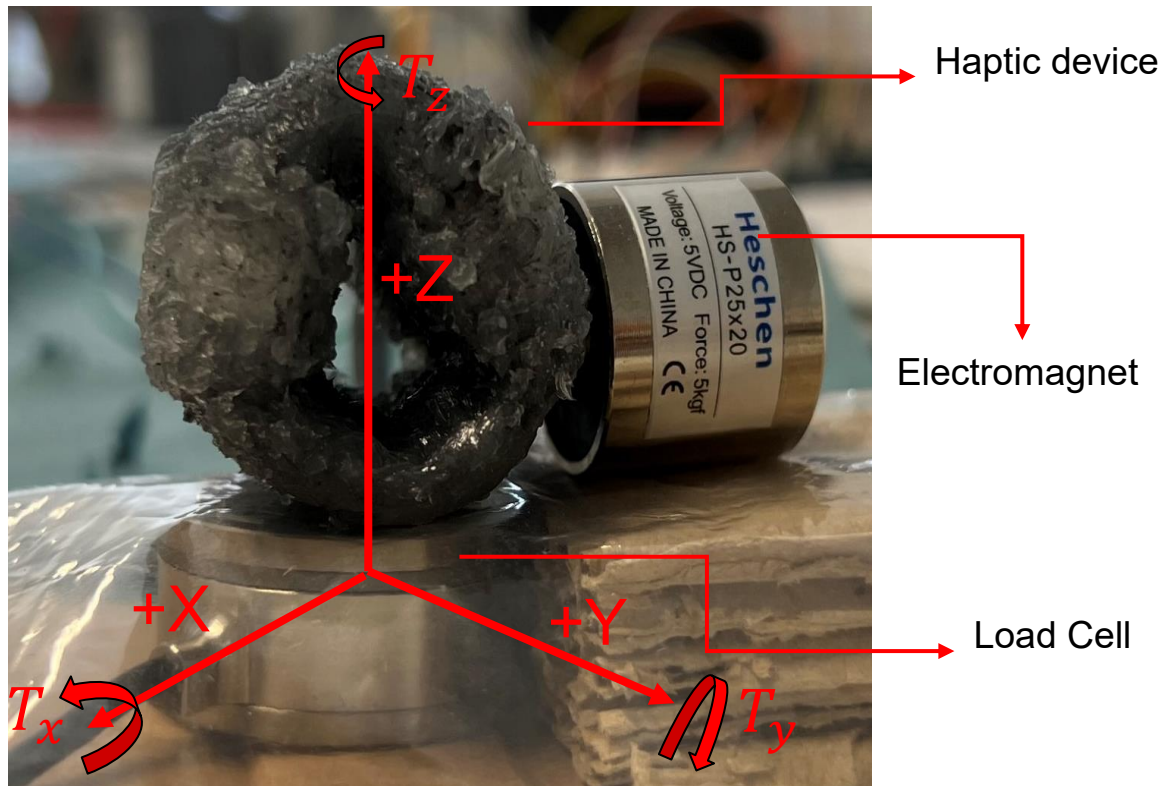


Figure 22: Experimental Setup

The +X, +Y, and +Z signs indicate the positive X, Y and Z axis of the load cell sensor. The electromagnet is placed such that the magnetic field generated is perpendicular to the direction of the Magnetorheological fluid. Torque generated in the anti-clockwise direction in the X, Y and Z direction is considered as positive rotation. The activation frequency selected for this test are 1Hz, 1.25Hz, 1.66Hz, 2.5 Hz and 5Hz. The figure below shows the results for various step size.

## Results

The normal force generation for various activation period are presented below:

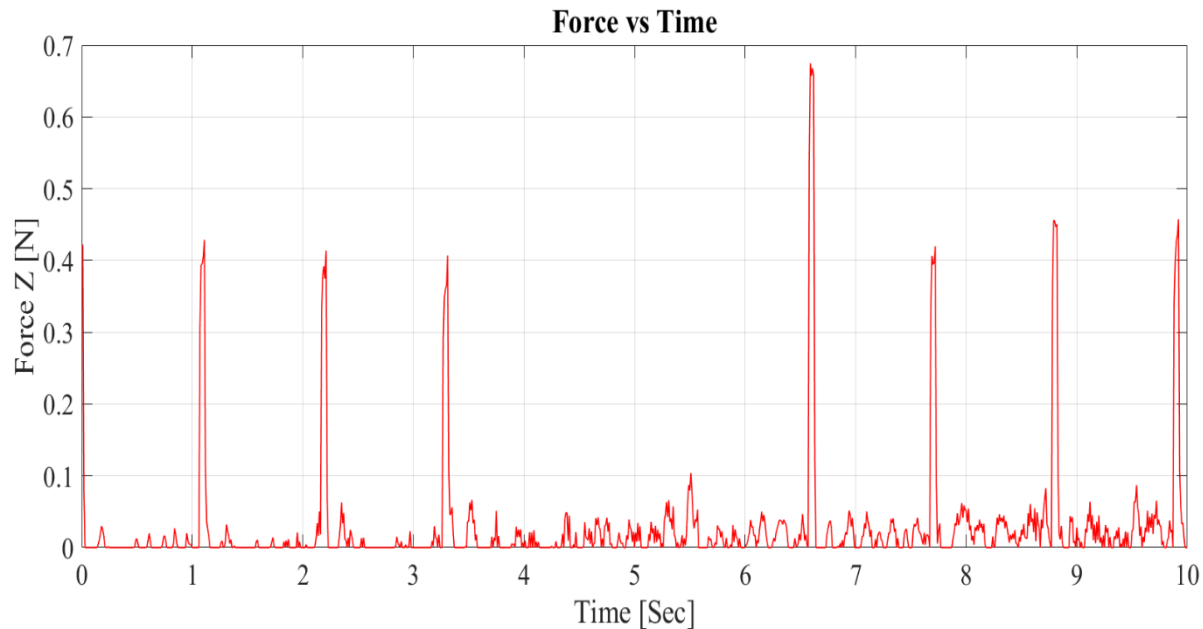


Figure 23: Frequency of 1 Hz

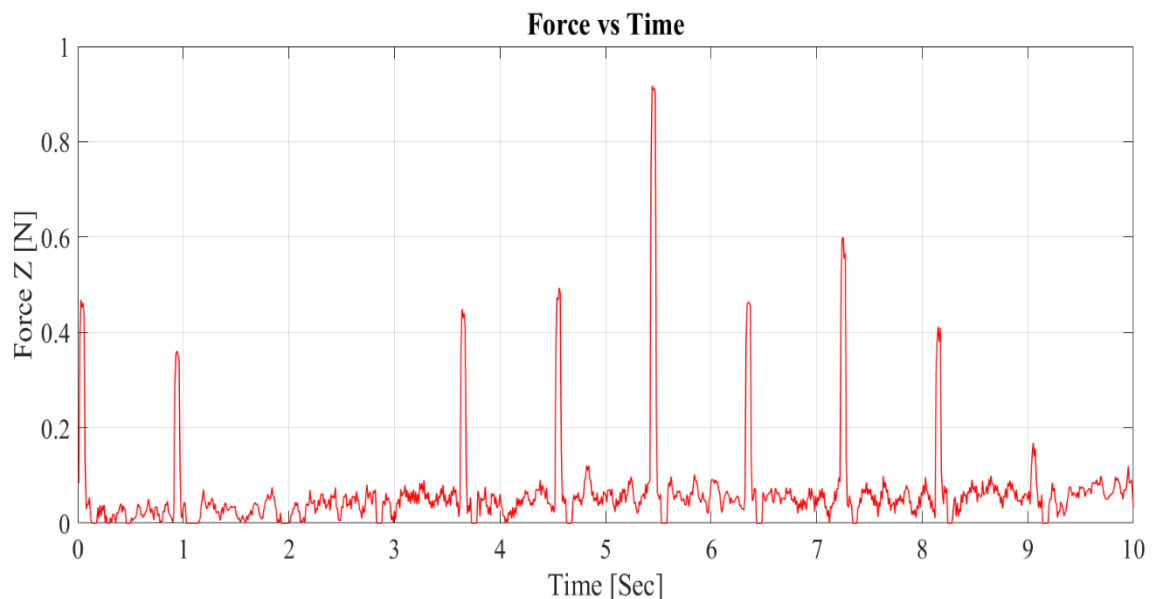
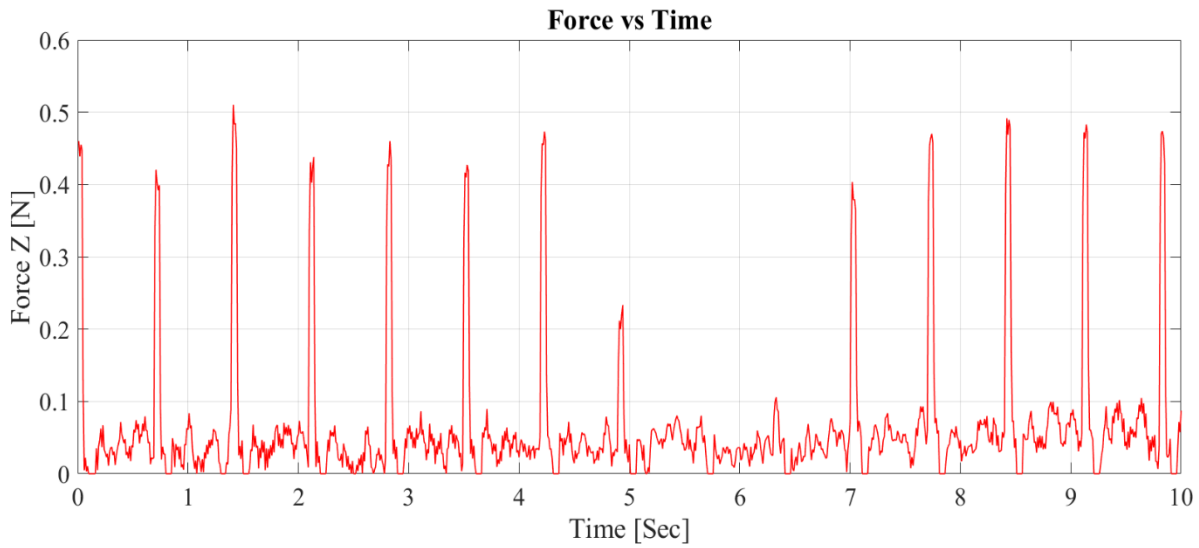
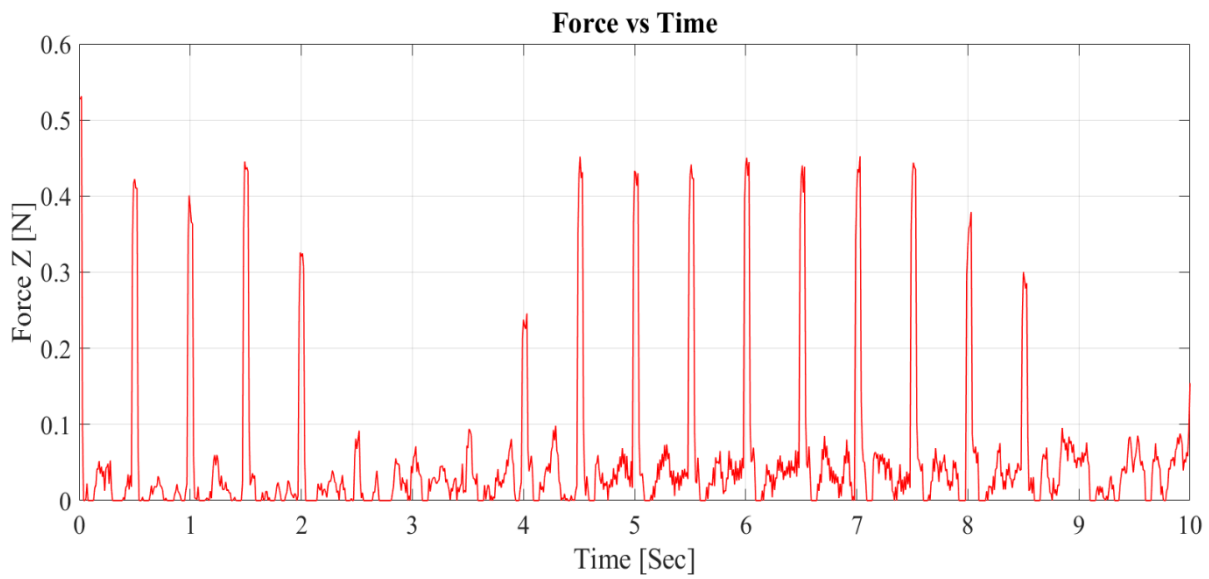


Figure 24: Frequency of 1.25Hz



*Figure 25: Frequency of 1.66Hz*



*Figure 26: Frequency of 2.5 Hz*

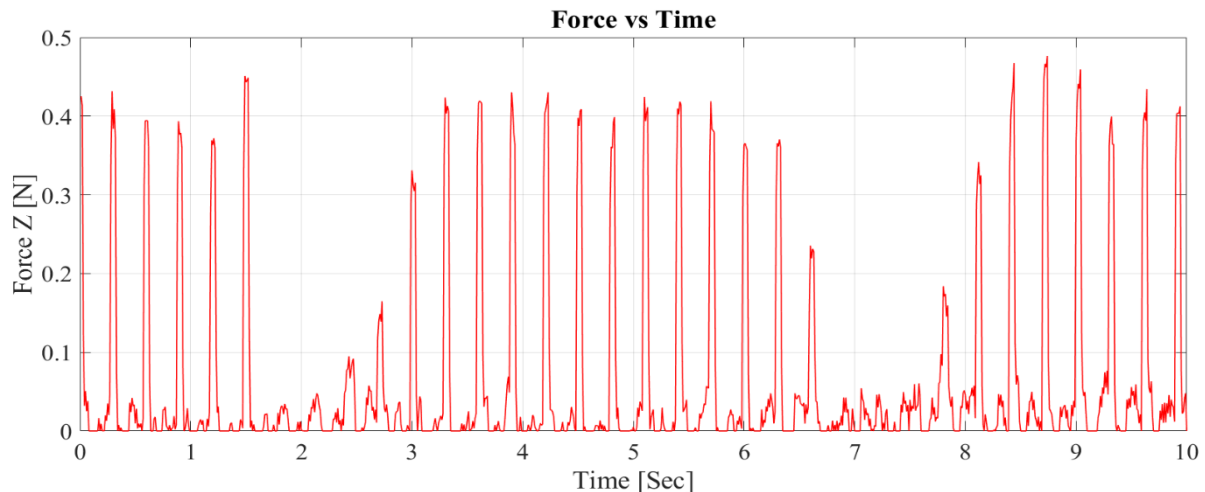


*Figure 27: Frequency of 5Hz*

The above graphs represent the magnitude of forces generated under different activation frequency values. The haptic device was placed such that the bottom skin will be in contact with the surface of the load cell sensor. Any pressure towards the face of the sensor will be captured as negative force in the Z axis. When the haptic device is actuated, the forces generated on the wall will on the outer sides of the hollow channels as represented in fig 21. Hence, the negative values in the Z axis were monitored and post processed for determining the absolute magnitude of force. Based on the graphs presented above, the following observations were noted:

- The average magnitude of force generated was 0.4 N
- The amplitude drops significantly after certain actuations.
- The magnitude of forces is not constant however remain around 0.4 N overall

The magnitude of force can be attributed to the strength of the electromagnet. The electromagnet used for this project generates a lifting force of 50N. A higher capacity magnet might result in increase in the magnitude. The drop in the amplitude is significant for lower frequencies but are less in number as the frequency increases. This indicated that the fluid is responsive for higher activation frequencies but performs poorly as the frequency decreases. Inconsistent amplitudes could be due to the quality of the suspended particles of the MR Fluids. A fluid with different particles and carrier fluid might provide consistent results.

#### Evaluation of Lateral forces

The lateral forces on the haptic device are generated when the forces generated by the chain formation is complemented by a pressure drop within the channels. The resultant is a force generated tangential to the fingers. A similar setup, as explained above, is used for evaluation.

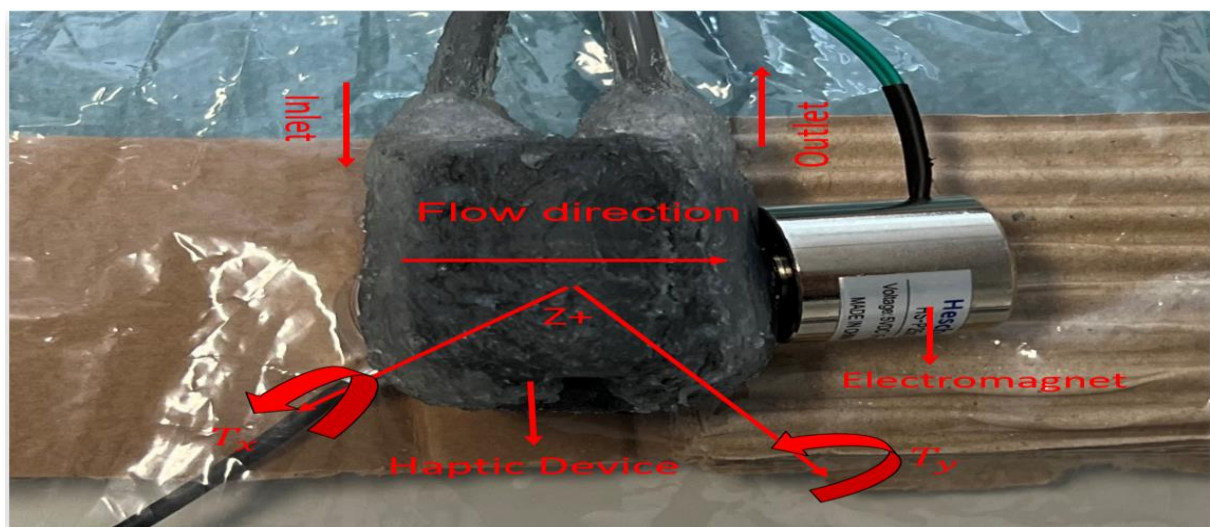


Figure 28: Experimental Setup

Figure 29 represents the various axis of the load cell sensor, the haptic device, and the electromagnet position for measuring the torque and force characteristics. The torque in X and Y axis of the load cell and the normal forces in the Z direction is evaluated. The Pump for this test is in the ON state allowing the fluid to flow from the inlet, around the finger through the top and bottom skins to the outlet. The load cell located on the bottom of the haptic device will capture the force and torque produced.

## Results

The Torque and normal forces generated under various activation frequency is illustrated below:

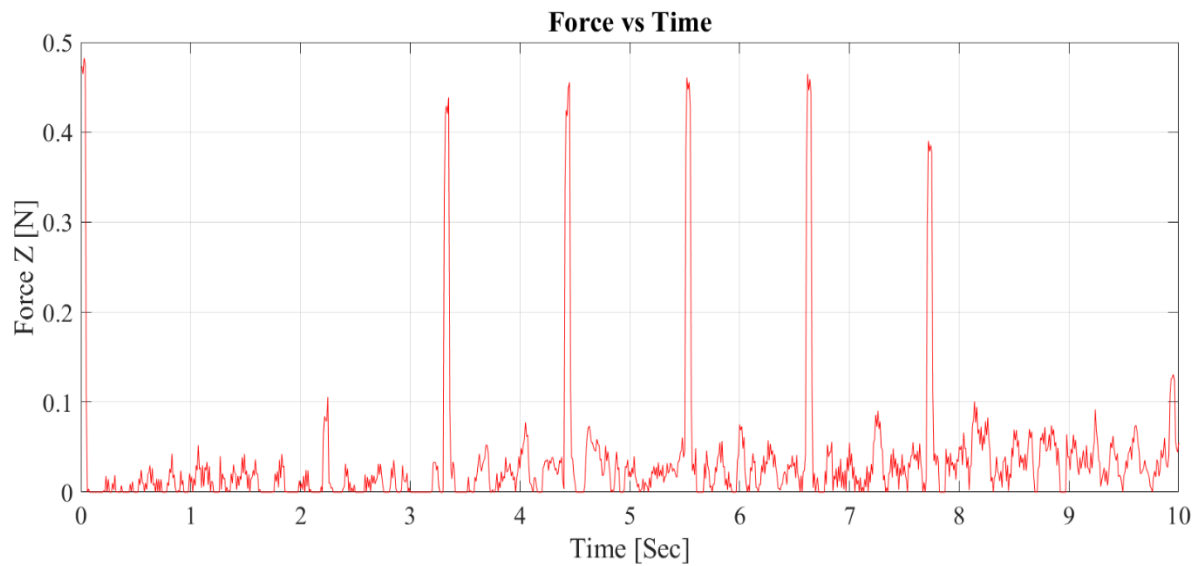


Figure 29: Frequency of 1HZ

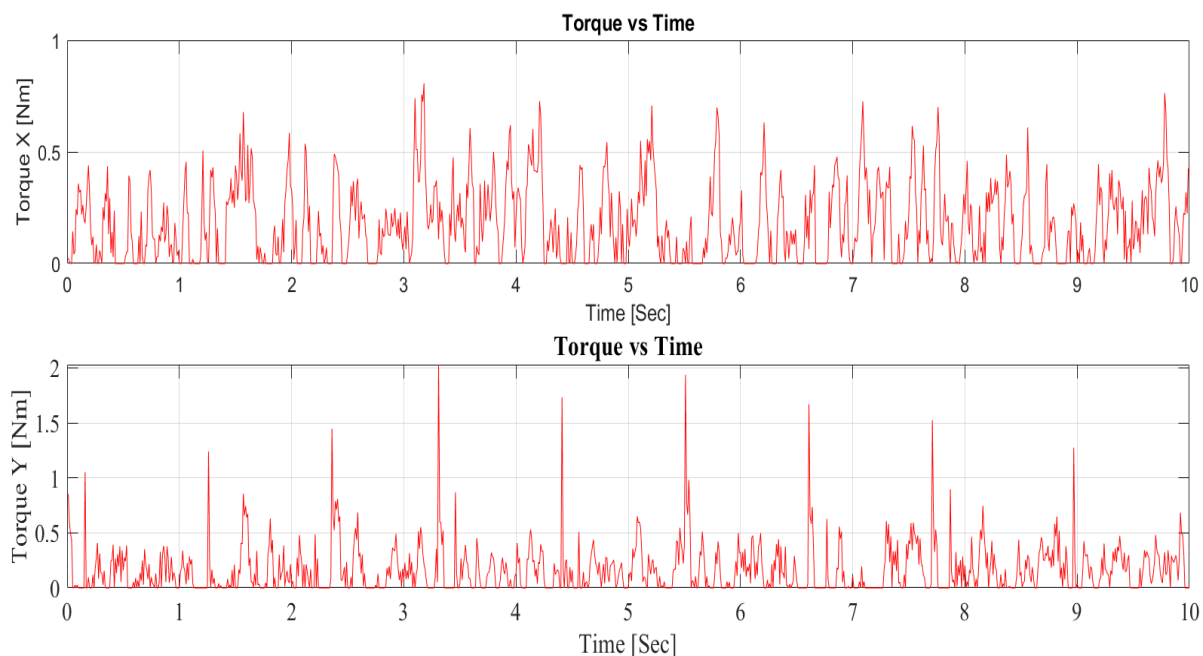


Figure 30: Frequency 1Hz

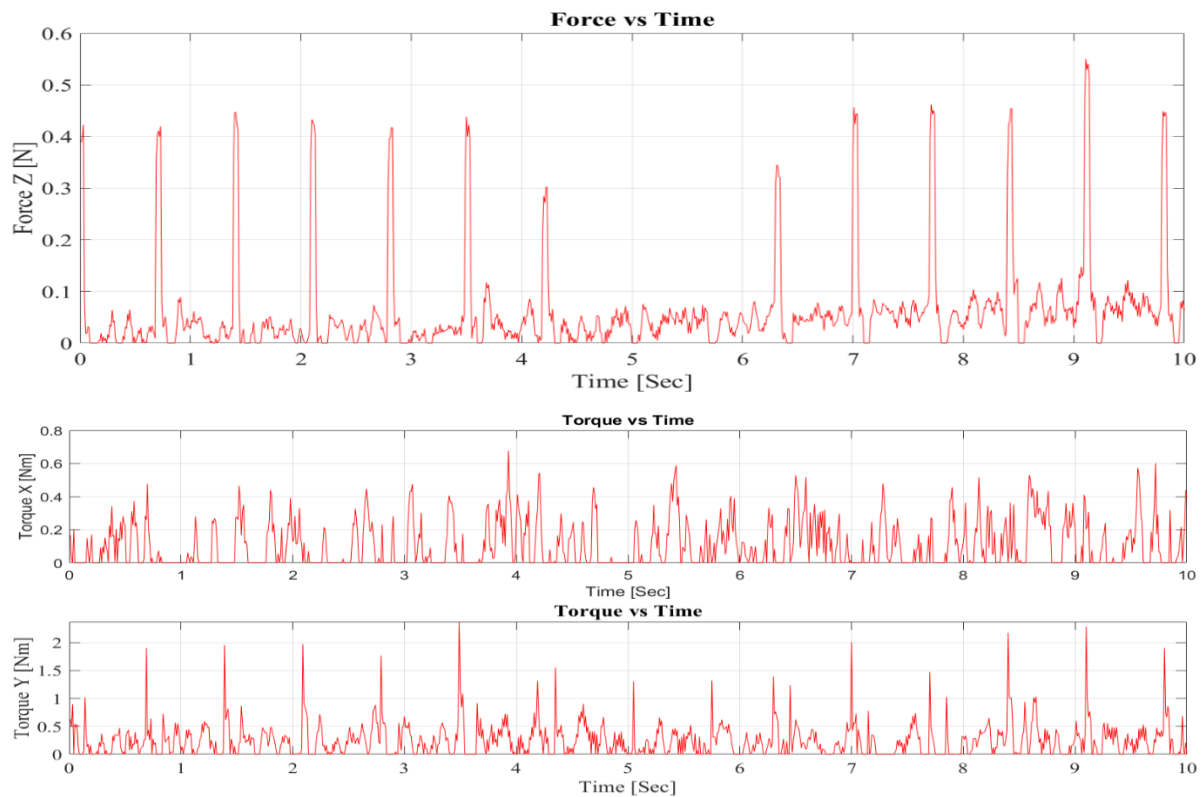


Figure 31: Frequency 1.66 Hz

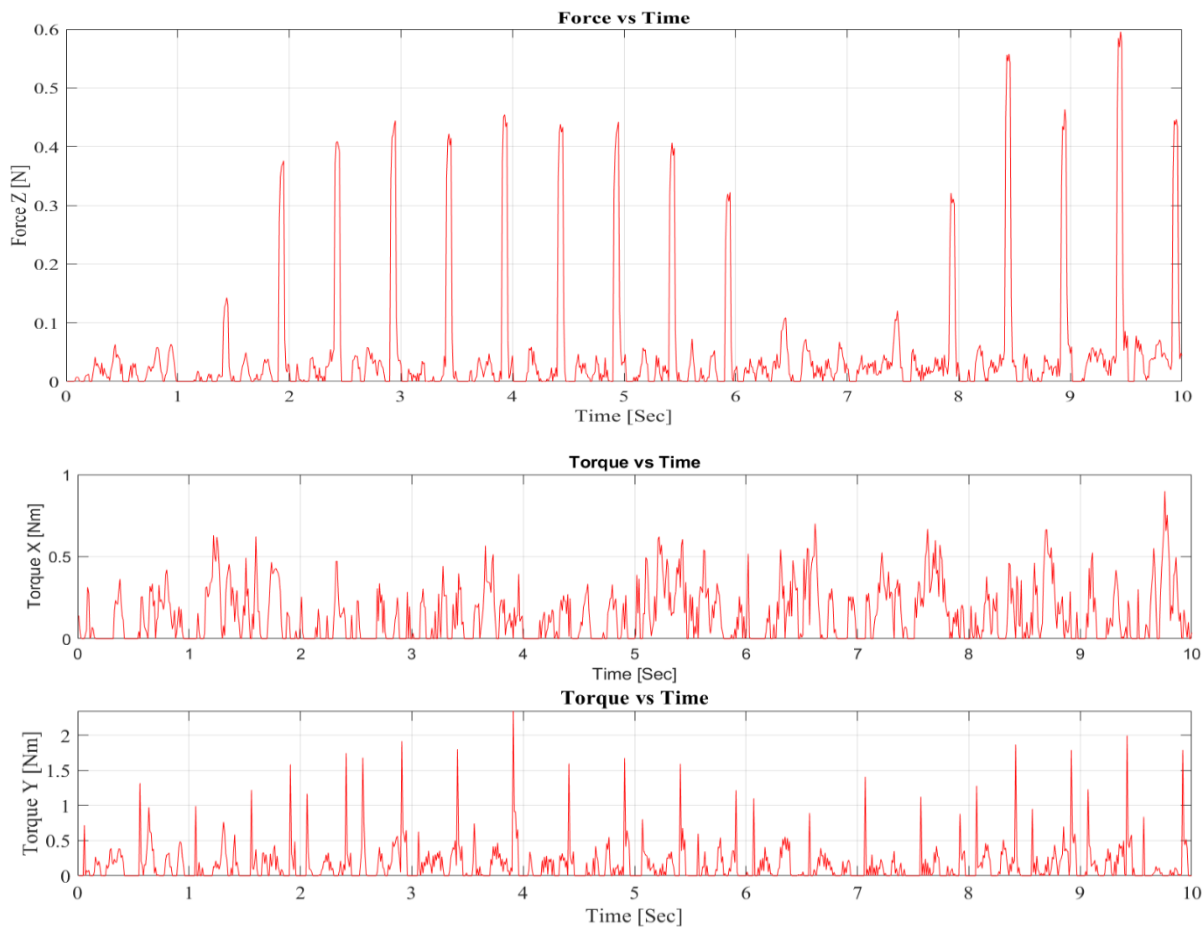
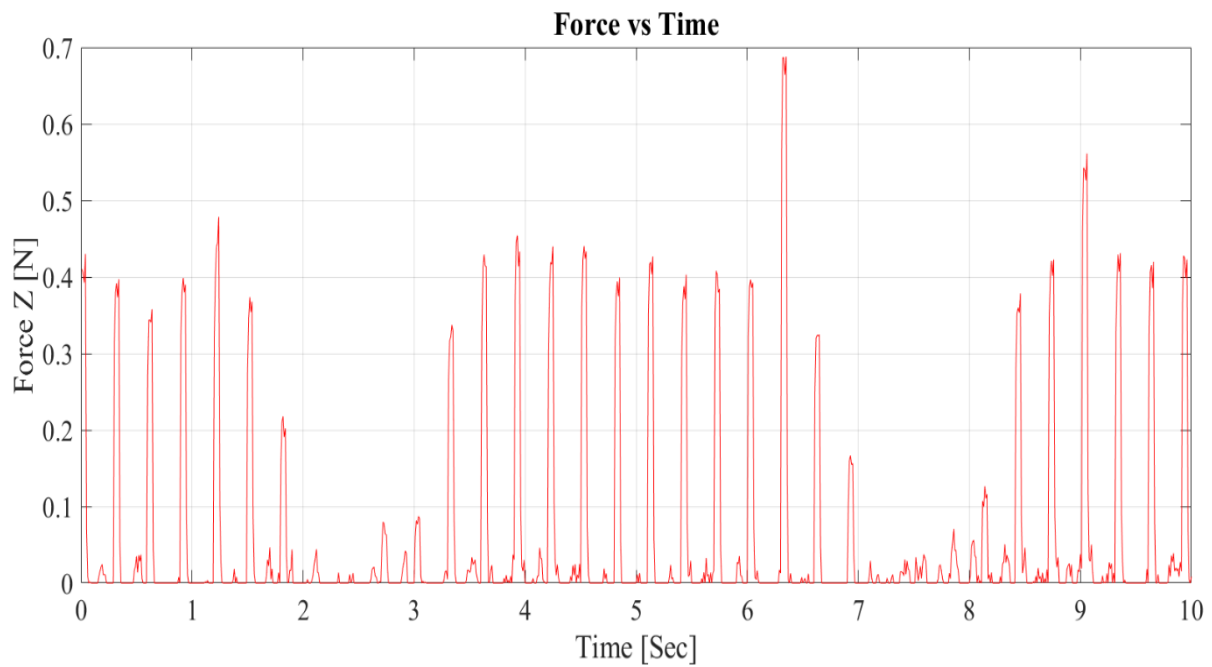
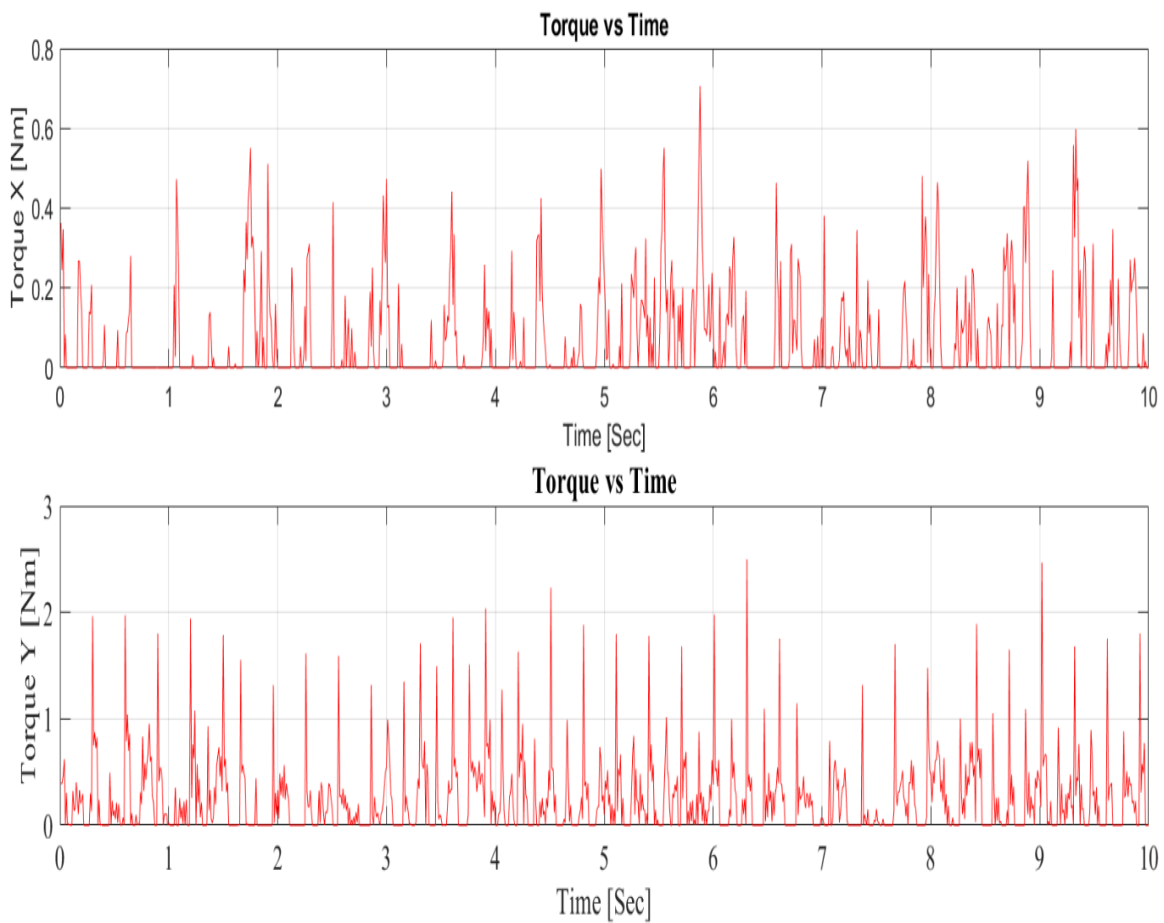


Figure 32: Frequency 2.5 Hz



*Figure 33: Frequency 5 Hz*



*Figure 34: Frequency 5Hz*

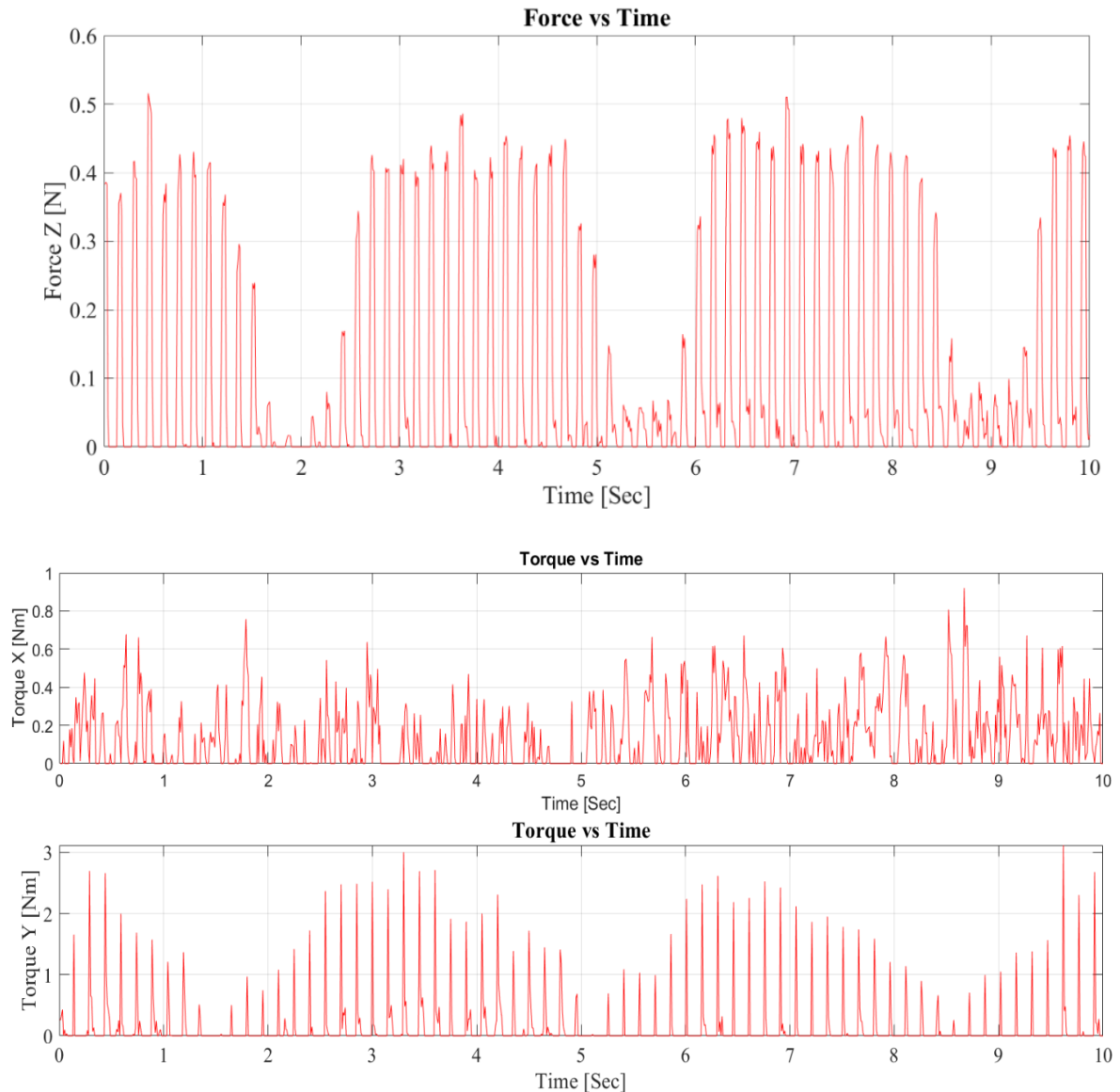


Figure 35: Frequency 20 Hz

The graph above shows the magnitude of Force and Torque capture for various activation frequency. Consistent with the results in the previous section, the normal forces generated have an average magnitude of 0.4N. The amplitude of forces is irregular with occasional dips. The torque value in the X axis fluctuates from 0.4Nm to 0.5Nm. The Y axis has a maximum amplitude of 2 Nm and has similar characteristic as the normal forces in Z direction. The cyclic dip in the amplitude can be attributed to the amount of fluid present in the activation region. It is possible that the flow rate across the inlet and the outlet of the haptic device is irregular which effects the torque and normal forces generated. It is also observed that for a frequency of 20Hz, the fluid fails to generate forces accordingly and is capped at 7Hz instead. This could

be attributed to the response time of the MRF-132DG. It is possible that after a certain threshold, the fluid fails to exhibit the MR effect.

## Developing a feedback system for a Franka Gripper

To evaluate the haptic feedback device under real life scenarios, a feedback system for a gripping task was performed. The gripper on a Franks Emika was utilized to complete this test. An FSR (Force Sensitive Resistor) sensor was attached to one end of the gripper such that it compresses when a gripping task is performed. The FSR is connected to an Arduino UNO, via an analog pin such that a signal is generated when pressure is applied on the FSR sensor. The FSR sensor is a resistive type device. One end of the sensor is connected to the 5V volt pin of the Arduino. The other side is divided into the ground pin and the analog input pin. The ground is connected via a 10K Ohm resistor. Under zero loading, the resistance on the FSR sensor is infinite. As the load on the sensor increases, the resistance value decreases generating an analog signal. The drop in the resistance value is corresponding to the applied pressure on the sensor.

The Image below shows the overall setup:

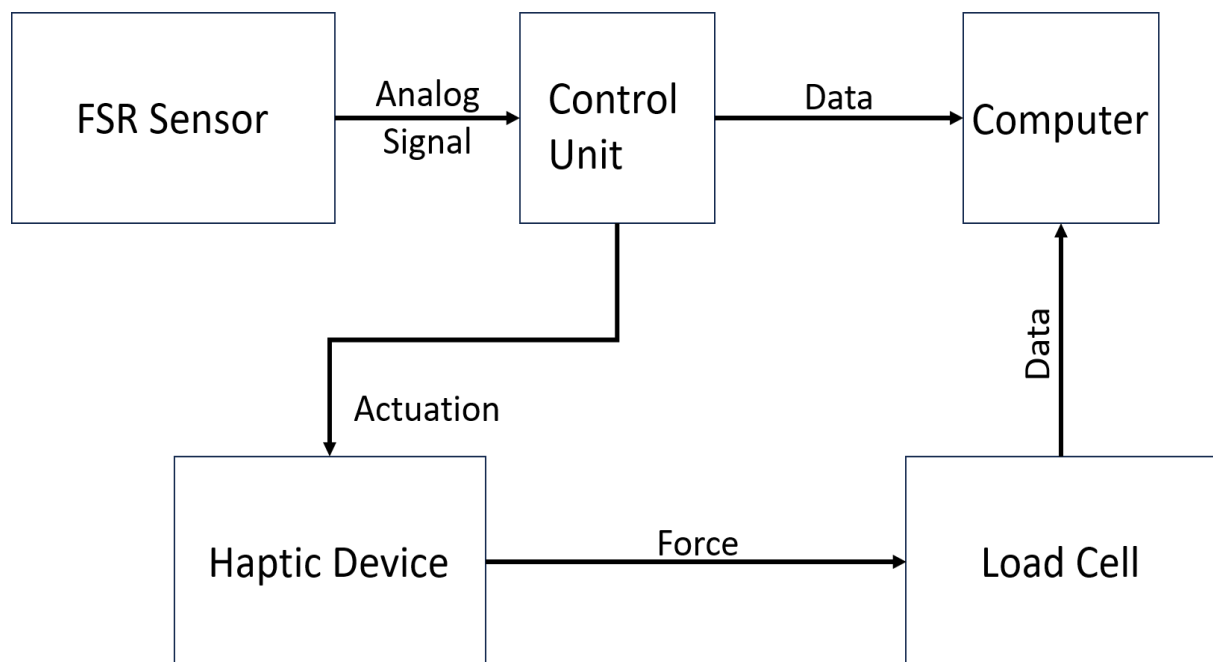


Figure 36: Haptic System Setup with FSR Sensor

The complete feedback system consists of an FSR sensor mounted on the gripper of a Franka arm, a control unit to send and receive signals, the haptic device, a 6-axis load cell sensor, and a windows Linux operating system-based computer. On receiving appropriate signals from the FSR sensor, the control unit processes the information and provides actuation to the haptic

device. The control unit also communicates to the computer in order to log data received from the FSR sensor. As the haptic system generates force, the load cell sensor captures the magnitude and transfers the data to the computer.

The Gripper on the Franks Emika's arm, can produce 20N to 80N of gripping force. The FSR sensor used for this project can sense forces up to 100N. The figure below represents the sensor setup on the gripper.



Figure 37: The FSR Sensor and the Franka Gripper

To ensure the FSR sensor is in maximum contact with the object to be gripped, the sensor is placed on a uniform rectangular plate which is mounted on one side of the end effector. The Object used for the gripping task is a plastic rectangular flat plate. The plate has a length of 100 mm and a uniform cross-section. The images below represent the plate:

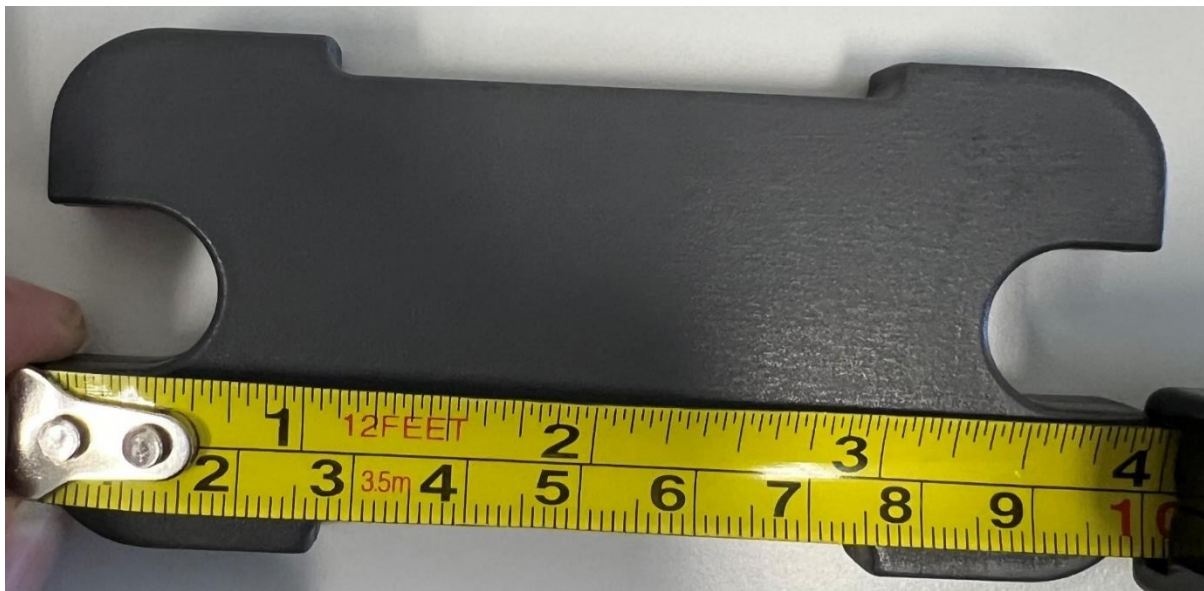


Figure 38: Rectangle Plate

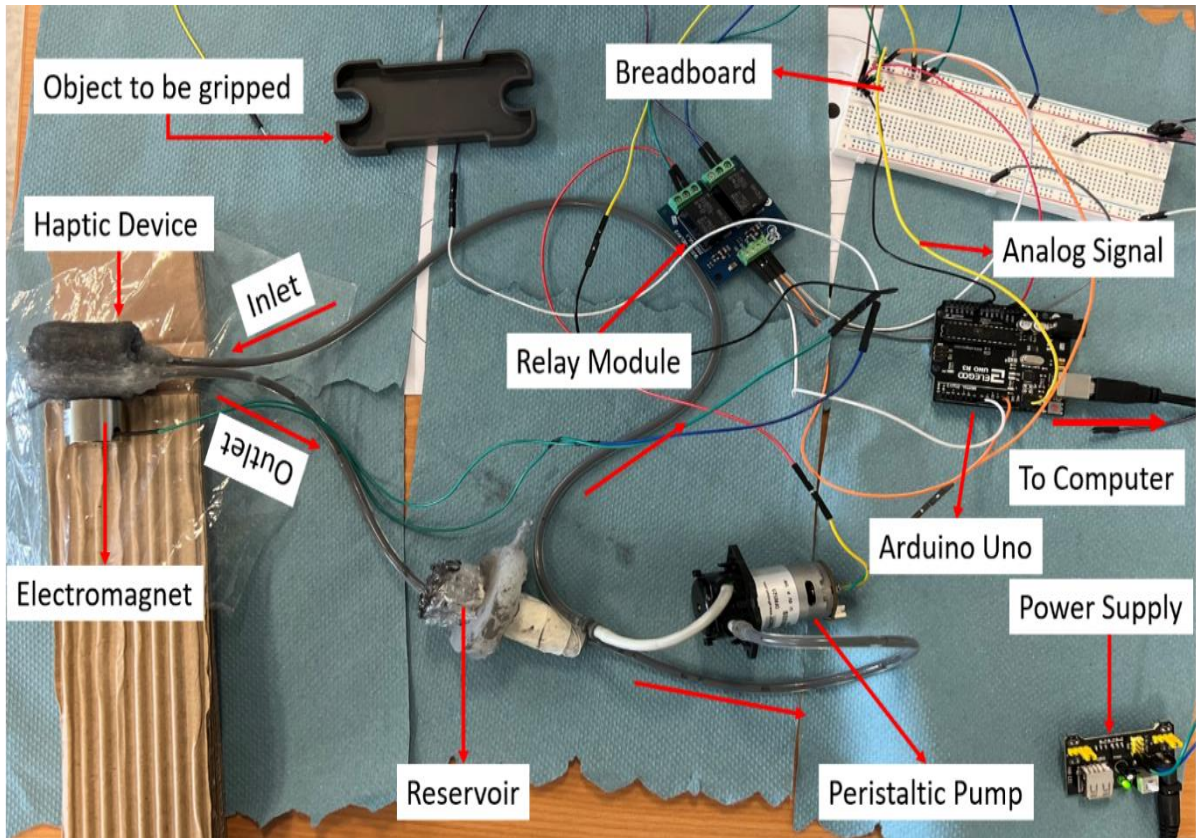
To determine the analog values generated by the FSR for different gripping strength, the plastic plate was gripped with varying magnitude of force using the Franks Gripper. The table below represents the results:

Table 3: Analog Values for various gripping Force

Force [N]	Analog Signal Range [0-1023]
20N	300-329
30N	330-360
40N	362-390
50N	395-425
60N	430-460
70N	465-495
80N	500-530

The feedback for the gripping task was mapped to generate varying pulse by the Haptic device. As the magnitude of the gripping force changes, the resistance on the FSR sensor will change. This change was mapped to the activation frequency of the electromagnet. When the gripping forces are low, the number of pulses generated by the device will be less. As the magnitude of the gripping force increases, the frequency of the pulse increases. The main intention behind this task is to generate feedback which informs about the gripping force of an object. The gripping task was done for three values of force; 20N, 50N and 80N. The signals generated by the FSR sensor and the loadcell sensor were logged. The sampling rate for both the sensors was

20Hz. The total duration for each gripping task was 30 Sec. The physical setup of the FSR sensor, the haptic device and other components are presented in the figure 40:



*Figure 39: The Physical Setup for Gripping Task*

The setup illustrated in Fig 40, is used for capturing the forces generated by the haptic device and the FSR sensor. In the above figure, the yellow wire to the Arduino uno, represented by “Analog Signal,” is used for receiving signal from the FSR sensor. The analog signal is processed by the Arduino uno and is transferred using USB communication. To capture the data from the FSR sensor, the ROS Serial protocol was used. The analog signal received on the Arduino Uno was echoed to the terminal window and was captured to a CSV file. Appendix-A illustrates the same. Using the values from Table-2, the appropriate analog value was selected to actuate the haptic device. For a gripping force of 20N, the actuation frequency was set to 1Hz. For 50N and 80N, the frequency was increased to 2Hz and 10 Hz respectively.

## Results

The graphs below show the FSR sensor values against the load cell sensor values. Each gripping task is performed for 30 Seconds.

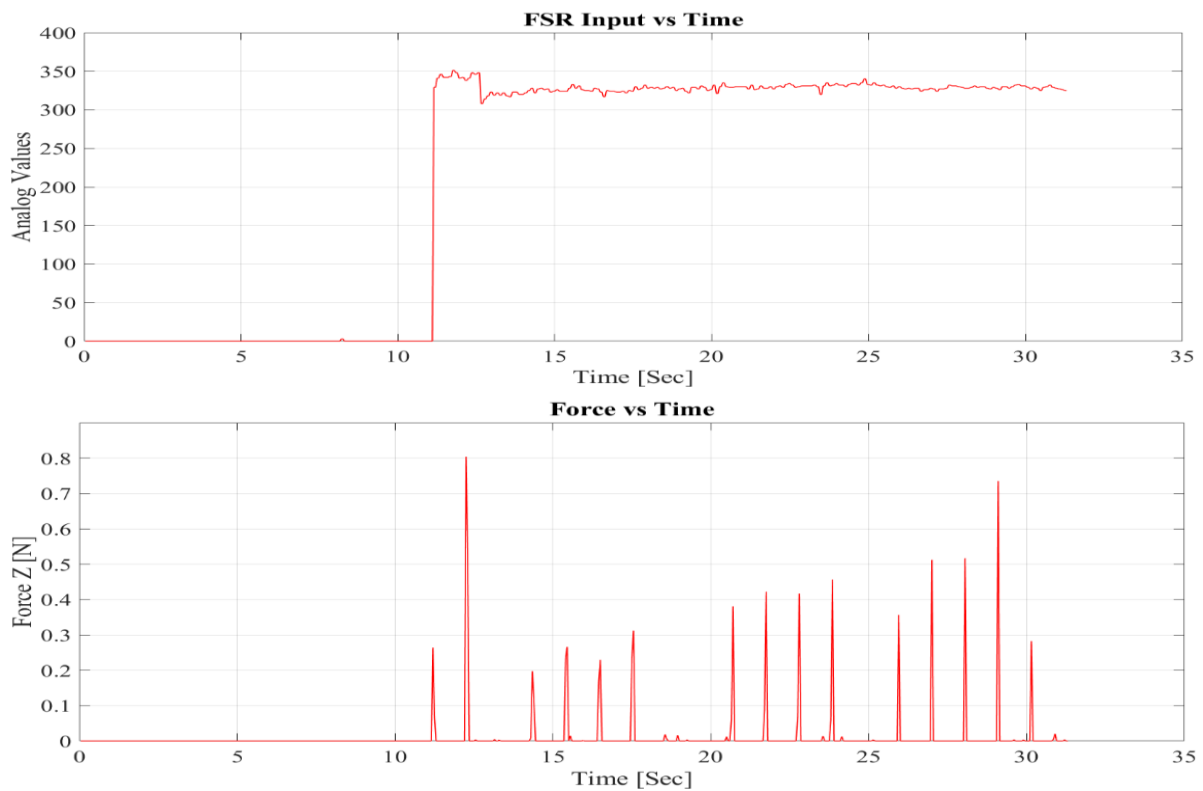


Figure 40: FSR sensor and Load cell sensor values corresponding to 20N gripping Force

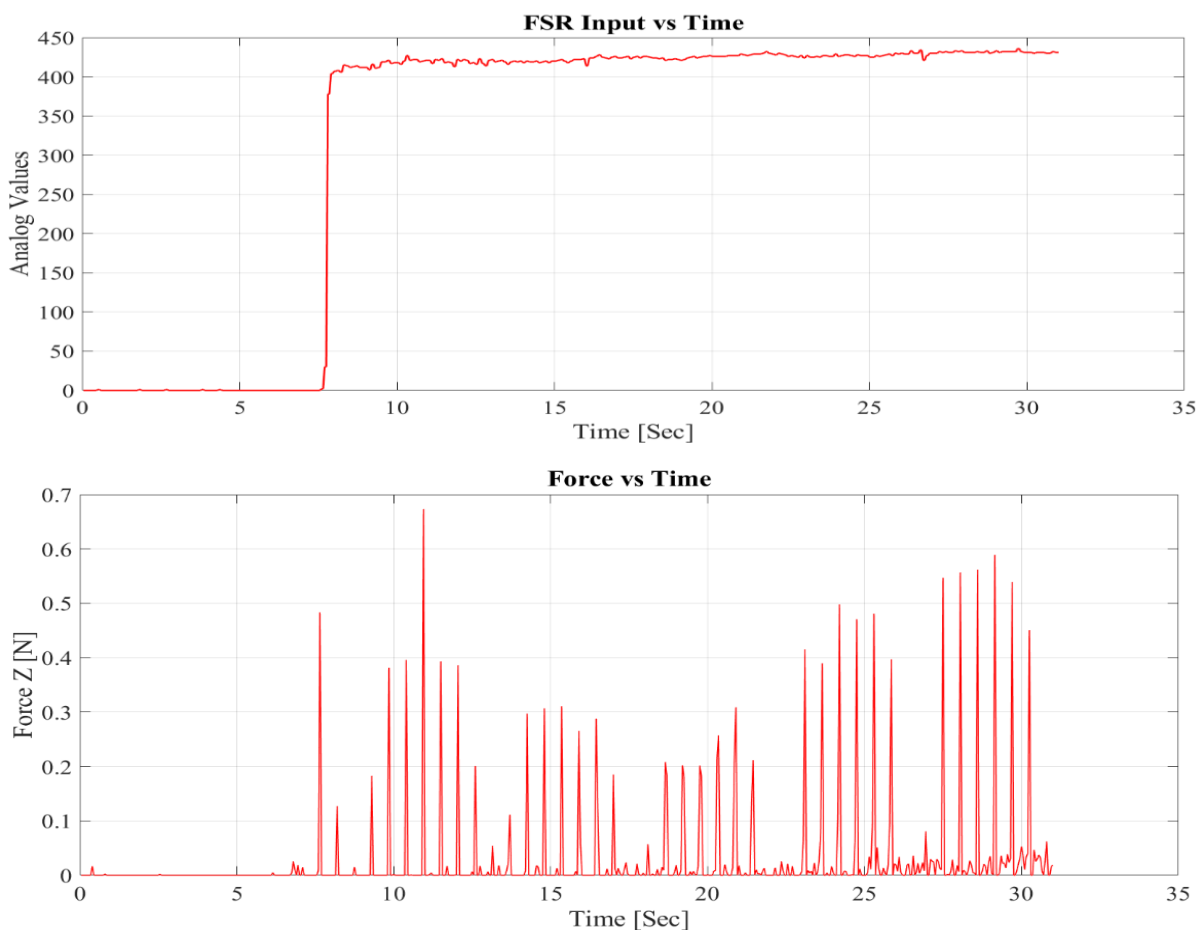


Figure 41: FSR sensor and Load cell sensor values corresponding to 50N gripping Force

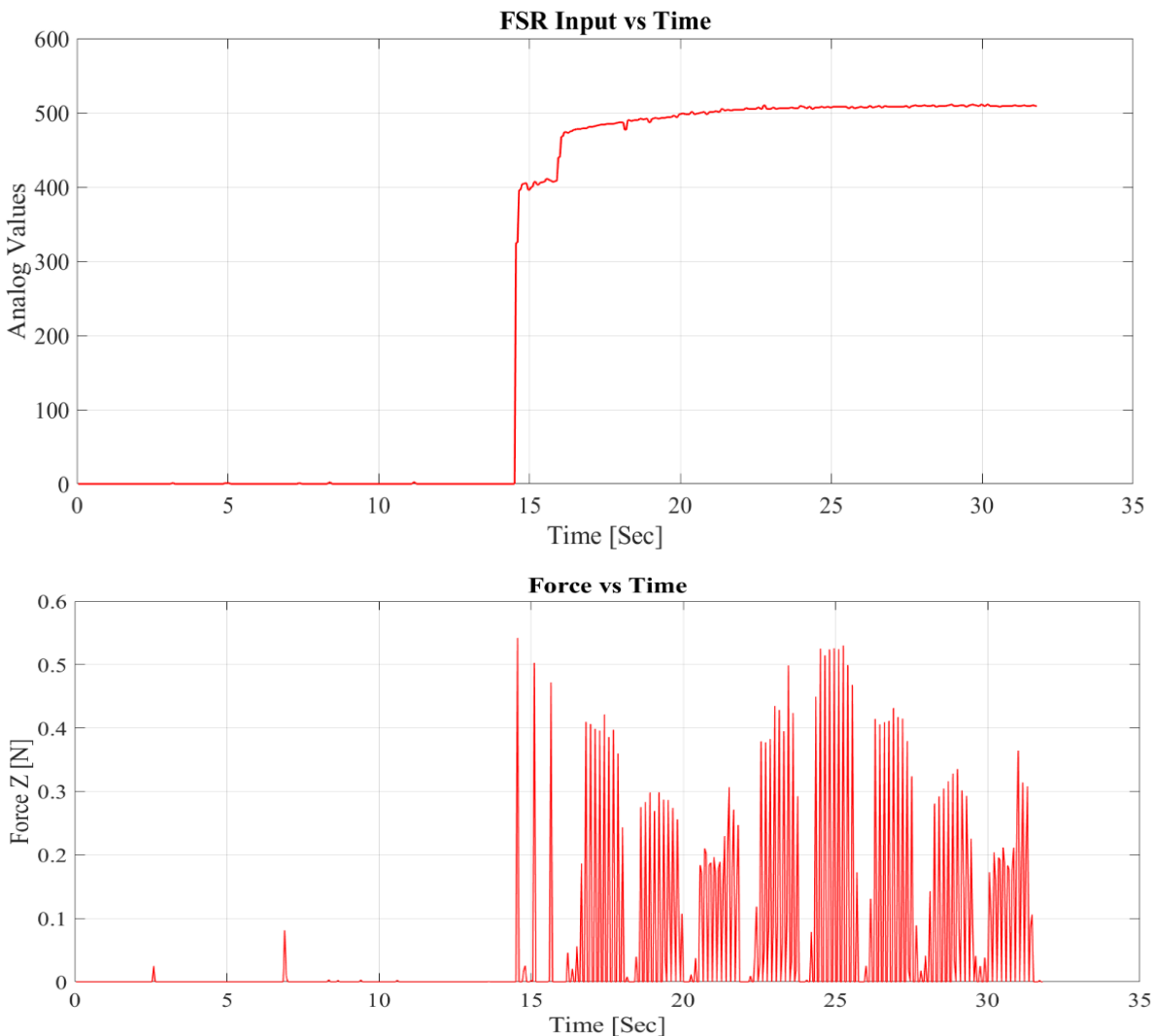


Figure 42: FSR sensor and Load cell sensor values corresponding to 80N gripping Force

The graph corresponding the FSR sensor analog values show a sudden rise in the amplitude after staying zero for initial few seconds. The sudden spike represents the gripping action. It can be observed from the above graphs that the responsiveness of the haptic system is quick. It is evident from the Fig 41, 42 and 34, that the haptic system instantly generates force as the FSR sensor senses a change in resistance. However, as stated in previous section, irregular amplitude and drastic drop in amplitude is consistent with this test too.

## Conclusion and Future Work

This thesis has delved into the development of a tactile feedback system centered on Magnetorheological (MR) Fluid, designed to produce cutaneous forces through a wearable haptic device. Initially, the device's construction involved two separate layers of silicone skin, resulting in encountered issues such as deformation and the presence of air bubbles. Additionally, assembly challenges were identified, prompting an alternative approach in which

both the top and bottom skin layers were cast together, effectively dividing the haptic system into two separate sets of casts.

An inlet/outlet port with distribution channels, manufactured using 3D printing, was employed for MR Fluid distribution between the layers. To generate both normal and lateral forces on the glabrous skin of the fingers, the system incorporated a peristaltic pump, an electromagnet, a relay module, and an Arduino. The electromagnet's brief actuation produced detectable pulses by mechanoreceptors beneath human skin. Magnitude assessments of force and torque were executed using a Loadcell sensor. Evaluation of the system spanned various activation frequencies, revealing its capacity to generate normal force of 0.4N and torques of 0.5Nm and 2Nm in the X and Y axes, respectively.

Considering the pulse-based nature of the system, higher frequencies yielded continuous feedback, whereas lower frequencies resulted in less favourable outcomes. Despite its swift response, the system exhibited inconsistency in force amplitudes when integrated with a Franka gripper for gripping tasks.

Although this tactile feedback system was tailored for gripping tasks, its applicability spans diverse domains. Customizing magnetic field intensity and pulse frequency opens avenues for adapting the system for tasks including grasping, edge detection, collision avoidance, and slip detection within virtual environments and teleoperation scenarios. In the medical field, it can emulate tactile feedback during catheter insertion and assist in identifying potential risks within the urethra.

Moreover, the system has the capability to simulate human pulse, proving invaluable for medical training. Its portability and ease of implementation, owing to its silicone rubber-based design, distinguish it from existing pulse simulators. Within the gaming industry, the system's adaptability permits the provision of rich haptic feedback, surpassing the limited feedback capabilities of conventional vibration motors in gaming consoles.

Looking ahead, exploring alternative design approaches for the wearable device and adjusting parameters such as magnetic intensity, pump size, and activation area offer potential enhancements in force generation. Integration of multiple electromagnets could facilitate the creation of multiple actuation sites, enabling the simulation of corners and collisions in VR environments and teleoperation tasks.

## References

1. J. Dargahi and S. Najarian, "Human tactile perception as a standard for artificial tactile sensing—a review," *The International Journal of Medical Robotics and Computer Assisted Surgery*, vol. 1, no. 1, pp. 23–35, Jun. 2004, doi: <https://doi.org/10.1002/rcs.3>.
2. "The sense of Touch in wine tasting," WINE FOR SOUL, May 04, 2013. <https://wine4soul.com/2013/05/04/oral-touch-and-wine-tasting/> (accessed Sep. 02, 2023).
3. A. Tzemanaki, G. A. Al, C. Melhuish, and S. Dogramadzi, "Design of a Wearable Fingertip Haptic Device for Remote Palpation: Characterisation and Interface with a Virtual Environment," *Frontiers in Robotics and AI*, vol. 5, Jun. 2018, doi: <https://doi.org/10.3389/frobt.2018.00062>.
4. H. Z. Tan, S. Choi, F. W. Y. Lau, and F. Abnousi, "Methodology for Maximizing Information Transmission of Haptic Devices: A Survey," *Proceedings of the IEEE*, vol. 108, no. 6, pp. 945–965, Jun. 2020, doi: <https://doi.org/10.1109/jproc.2020.2992561>.
5. Yoon Kwon Nam, M. K. Park, and R. Yamane, "Smart glove: hand master using magnetorheological fluid actuators," *Proceedings of SPIE*, Dec. 2007, doi: <https://doi.org/10.1117/12.783776>.
6. S. H. Winter and M. Bouzit, "Use of Magnetorheological Fluid in a Force Feedback Glove," *IEEE Transactions on Neural Systems and Rehabilitation Engineering*, vol. 15, no. 1, pp. 2–8, Mar. 2007, doi: <https://doi.org/10.1109/tnsre.2007.891401>.
7. G. Liu, F. Gao, D. Wang, and W.-H. Liao, "Medical applications of magnetorheological fluid: a systematic review," *Smart Materials and Structures*, vol. 31, no. 4, p. 043002, Mar. 2022, doi: <https://doi.org/10.1088/1361-665x/ac54e7>.
8. Y. Song et al., "Design and performance evaluation of a haptic interface based on MR fluids for endovascular tele-surgery," *Microsystem Technologies*, vol. 24, no. 2, pp. 909–918, Apr. 2017, doi: <https://doi.org/10.1007/s00542-017-3404-y>.
9. M. Eaton, J.-H. Koo, T.-H. Yang, and Y.-M. Kim, "Simulating Age Related Radial Pulses Using Magneto-Rheological Fluids," Sep. 2022, doi: <https://doi.org/10.1115/smasis2022-90793>.
10. J.-H. Koo, T. Tantiyartyanontha, Y.-M. Kim, H. Kang, and T.-H. Yang, "Application of magneto-rheological fluids for generating a wide range of radial pulse waveforms,"

Smart Materials and Structures, vol. 27, no. 12, p. 125010, Nov. 2018, doi: <https://doi.org/10.1088/1361-665x/aaeaa7>.

11. J. Graham, S. G. Manuel, M. S. Johannes, and R. S. Armiger, “Development of a multi-modal haptic feedback system for dexterous robotic telemanipulation,” Oct. 2011, doi: <https://doi.org/10.1109/icsmc.2011.6084219>.
12. R. L. Pierce, E. A. Fedalei, and K. J. Kuchenbecker, “A wearable device for controlling a robot gripper with fingertip contact, pressure, vibrotactile, and grip force feedback,” Feb. 2014, doi: <https://doi.org/10.1109/haptics.2014.6775428>.
13. S. B. Schorr and A. M. Okamura, “Three-Dimensional Skin Deformation as Force Substitution: Wearable Device Design and Performance During Haptic Exploration of Virtual Environments,” IEEE Transactions on Haptics, vol. 10, no. 3, pp. 418–430, Jul. 2017, doi: <https://doi.org/10.1109/toh.2017.2672969>.
14. Sachille Atapattu, N. M. Senevirathna, H. Shan, Thanuja Madusanka, Thilina Dulantha Lalitharatne, and Damith Suresh Chathuranga, “Design and development of a wearable haptic feedback device to recognize textured surfaces: Preliminary study,” Jul. 2017, doi: <https://doi.org/10.1109/aim.2017.8013988>.
15. M. Gabardi, Massimiliano Solazzi, D. Leonardis, and A. Frisoli, “A new wearable fingertip haptic interface for the rendering of virtual shapes and surface features,” Apr. 2016, doi: <https://doi.org/10.1109/haptics.2016.7463168>.
16. H. Kim, M.-H. Kim, and W. Lee, “HapThimble,” May 2016, doi: <https://doi.org/10.1145/2858036.2858196>.
17. M. Zhu et al., “Haptic-feedback smart glove as a creative human-machine interface (HMI) for virtual/augmented reality applications,” Science Advances, vol. 6, no. 19, May 2020, doi: <https://doi.org/10.1126/sciadv.aaz8693>.
18. A. Tzemanaki, G. A. Al, C. Melhuish, and S. Dogramadzi, “Design of a Wearable Fingertip Haptic Device for Remote Palpation: Characterisation and Interface with a Virtual Environment,” Frontiers in Robotics and AI, vol. 5, Jun. 2018, doi: <https://doi.org/10.3389/frobt.2018.00062>.
19. A. T. Maereg, A. Nagar, D. Reid, and E. L. Secco, “Wearable Vibrotactile Haptic Device for Stiffness Discrimination during Virtual Interactions,” Frontiers in Robotics and AI, vol. 4, Sep. 2017, doi: <https://doi.org/10.3389/frobt.2017.00042>.
20. J. de Vicente, D. J. Klingenberg, and R. Hidalgo-Alvarez, “Magnetorheological fluids: a review,” Soft Matter, vol. 7, no. 8, p. 3701, 2011, doi: <https://doi.org/10.1039/c0sm01221a>.

21. M. R. Jolly, J. W. Bender, and J. D. Carlson, “Properties and Applications of Commercial Magnetorheological Fluids,” *Journal of Intelligent Material Systems and Structures*, vol. 10, no. 1, pp. 5–13, Jan. 1999, doi: <https://doi.org/10.1177/1045389x9901000102>.
22. O. Ashour, C. A. Rogers, and W. Kordonsky, “Magnetorheological Fluids: Materials, Characterization, and Devices,” *Journal of Intelligent Material Systems and Structures*, vol. 7, no. 2, pp. 123–130, Mar. 1996, doi: <https://doi.org/10.1177/1045389x9600700201>.
23. C. Loudon and K. McCulloh, “Application of the Hagen—Poiseuille Equation to Fluid Feeding through Short Tubes,” *Annals of the Entomological Society of America*, vol. 92, no. 1, pp. 153–158, Jan. 1999, doi: <https://doi.org/10.1093/aesa/92.1.153>.
24. B. C. Eu, “Generalization of the Hagen—Poiseuille velocity profile to non-Newtonian fluids and measurement of their viscosity,” *American Journal of Physics*, vol. 58, no. 1, pp. 83–84, Jan. 1990, doi: <https://doi.org/10.1119/1.16328>.
25. “LORD TECHNICAL DATA LORD TECHNICAL DATA.” Accessed: Sep. 05, 2023. [Online]. Available: [https://lordfulfillment.com/pdf/44/DS7015\\_MRF-132DGMRFluid.pdf](https://lordfulfillment.com/pdf/44/DS7015_MRF-132DGMRFluid.pdf)
26. “Dynamic Viscosity - an overview | ScienceDirect Topics,” www.sciencedirect.com. <https://www.sciencedirect.com/topics/chemistry/dynamic-viscosity#:~:text=Until%20the%20temperature%20of%20such>
27. X. Wang and F. Gordaninejad, “Flow Analysis of Field-Controllable, Electro- and Magneto-Rheological Fluids Using Herschel-Bulkley Model,” *Journal of Intelligent Material Systems and Structures*, vol. 10, no. 8, pp. 601–608, Aug. 1999, doi: <https://doi.org/10.1106/p4fl-l1el-yflj-btre>.
28. Characterization of Magnetorheological Finishing Fluid for Continuous Flow Finishing Process - Scientific Figure on ResearchGate. Available from: [https://www.researchgate.net/figure/Flow-curves-of-Bingham-Plastic-HerschelBulkley-and-Cassons-fluid-model-see-Chhabra-and\\_fig3\\_329306853](https://www.researchgate.net/figure/Flow-curves-of-Bingham-Plastic-HerschelBulkley-and-Cassons-fluid-model-see-Chhabra-and_fig3_329306853) [accessed 8 Sep, 2023]
29. Annika Björn, Paula Segura de La Monja, Anna Karlsson, Jörgen Ejlertsson and Bo H. Svensson (2012). Rheological Characterization, Biogas, Dr. Sunil Kumar (Ed.), ISBN: 978-953-51-0204-5, InTech, Available from: <http://www.intechopen.com/books/biogas/rheological-characterization>

30. "Quick 2 Relays," www.gravitech.us. <https://www.gravitech.us/quick2relays.html> (accessed Aug. 31, 2023).
31. "Gravity\_Digital\_Peristaltic\_Pump\_SKU\_DFR0523-DFRobot," wiki.dfrobot.com. [https://wiki.dfrobot.com/Gravity\\_Digital\\_Peristaltic\\_Pump\\_SKU\\_DFR0523](https://wiki.dfrobot.com/Gravity_Digital_Peristaltic_Pump_SKU_DFR0523) (accessed Aug. 31, 2023).

## Appendix-A

The code used to store the FSR sensor values and trigger the haptic device based on the input signals from the FSR sensor.

```
1. #include <ros.h>
2. #include <std_msgs/Int32.h>
3.
4. //ROS node handle
5. ros::NodeHandle nh;
6.
7. int channel_1 = 6;
8. int channel_2 = 9;
9. int LED = LED_BUILTIN;
10. int fsrAnalog = 0;
11. int fsrReading;
12. int fsrVoltage;
13. unsigned long fsrResistance;
14. unsigned long fsrConductance;
15. long fsrForce;
16.
17. //ros-publisher
18. std_msgs::Int32 msg;
19. ros::Publisher FSR_val("FSR_val", &msg);
20.
21. // the setup routine runs once when you press reset:
22. void setup() {
23.   // initialize the digital pin as an output.
24.   Serial.begin(9600);
25.   pinMode(channel_1, OUTPUT);
26.   pinMode(channel_2, OUTPUT);
27.   pinMode(LED, OUTPUT);
28.   nh.initNode();
29.   nh.advertise(FSR_val);
30. }
31.
32. // the loop routine runs over and over again forever:
33. void loop() {
34.   fsrReading = analogRead(fsrAnalog);
35.   fsrVoltage = map(fsrReading, 0, 1023, 0, 5000);
36.   // Serial.print("Analog reading = ");
37.   Serial.print(fsrReading);
38.   msg.data = fsrReading;
39.   FSR_val.publish(&msg);
40.   Serial.print(",");
41.
42.   if (fsrVoltage == 0) {
43.     Serial.println("0");
44.     msg.data = fsrReading;
45.     FSR_val.publish(&msg);
46.   } else {
47.     fsrResistance = 5000 - fsrVoltage;
48.     fsrResistance *= 1000;
49.     fsrResistance /= fsrVoltage;
50.     // Serial.print("FSR resistance in ohms = ");
51.     Serial.println(fsrResistance);
52.   }
53.
54.   if (fsrReading > 300 && fsrReading <= 329) {
55.     digitalWrite(channel_2, HIGH);
56.     delay(1000);
57.     digitalWrite(channel_2, LOW);
58.   } else if (fsrReading > 395 && fsrReading <= 425) {
59.     digitalWrite(channel_2, HIGH);
60.     delay(500);
61.     digitalWrite(channel_2, LOW);
```

```
62. } else if (fsrReading > 500) {  
63.   digitalWrite(channel_2, HIGH);  
64.   delay(100);  
65.   digitalWrite(channel_2, LOW);  
66. }  
67. msg.data = fsrReading;  
68. FSR_val.publish(&msg);  
69. nh.spinOnce();  
70. delay(50);  
71. }
```

## Self-Review

This project was a unique opportunity to dive into the fascinating world of haptic systems and MR Fluids. The journey began with an extensive dive into the existing literature, where I delved deep into the intricate landscape of available haptic technology and MR Fluid-based devices. Along the way, I had the chance to acquire a host of new skills that were instrumental in achieving our project goals. From mastering the art of creating 3D-printed Molds to experimenting with silicone rubber casting and getting hands-on experience with microcontrollers for electronics control, this project expanded my skill set in unexpected ways.

However, as with any journey, this one had its fair share of challenges. One of the most persistent issues we faced was the device's susceptibility to leaks. Our initial attempts to address this problem using a combination of silicone rubber and super glue proved to be ineffective. It was only after conducting some research that we stumbled upon a solution in the form of silicone adhesive, which finally put an end to our leakage woes.

This project pushed me out of my comfort zone in the best possible way. With no prior background in haptic technology or MR Fluids, I found myself both exhilarated and daunted at times. But as we successfully achieved our project objectives, I gained a newfound sense of confidence in my ability to conduct independent research. Additionally, it put my time management and report-taking skills to the test, underscoring the importance of striking a balance between hands-on work and documentation to ensure everything progressed smoothly and on schedule.